

Secrecy Rate of the Cooperative RSMA-Aided UAV Downlink Relying on Optimal Relay Selection

Hamed Bastami, Majid Moradikia, Hamid Behroozi, *Member, IEEE*, and Lajos Hanzo, *Life Fellow, IEEE*

Abstract—The Cooperative Rate-Splitting (CRS) scheme, proposed evolves from conventional Rate Splitting (RS) and relies on forwarding a portion of the RS message by the relaying users. In terms of secrecy enhancement, it has been shown that CRS outperforms its non-cooperative counterpart for a two-user Multiple Input Single Output (MISO) Broadcast Channel (BC). Given the massive connectivity requirement of 6G, we have generalized the existing secure two-user CRS framework to the multi-user framework, where the highest-security users must be selected as the relay nodes. This paper addresses the problem of maximizing the Worst-Case Secrecy Rate (WCSR) in a UAV-aided downlink network where a multi-antenna UAV Base-Station (UAV-BS) serves a group of users in the presence of an external eavesdropper (*Eve*). We consider a practical scenario in which only imperfect channel state information of *Eve* is available at the UAV-BS. Accordingly, we conceive a robust and secure resource allocation algorithm, which maximizes the WCSR by jointly optimizing both the Secure Relaying User Selection (SRUS) and the network parameter allocation problem, including the RS transmit precoders, message splitting variables, time slot sharing and power allocation. To circumvent the resultant non-convexity owing to the discrete variables imposed by SRUS, we propose a two-stage algorithm where the SRUS and network parameter allocation are accomplished in two consecutive stages. With regard to the SRUS, we study both centralized and distributed protocols. On the other hand, for jointly optimizing the network parameter allocation we resort to the Sequential Parametric Convex Approximation (SPCA) algorithm. Our numerical results show that the proposed solution significantly outperforms the existing benchmarks for a wide range of network loads in terms of the WCSR.

Index Terms—Rate-splitting, Physical layer security, Robust beamforming, Secure relay selection, Imperfect CSIT, Worst-case optimization, Cellular UAV networks.

I. INTRODUCTION

6G wireless communications are envisioned to support the heterogeneous services of a massive number of connected users with ultra-reliability, e.g., $1000\times$ higher mobile data volume per geographical area, as well as $10 \sim 100\times$ more connected devices, offered at efficient resources usage [1], [2]. These indicative parameters are known as Key Performance Indicators (KPIs) of 6G. Upon growing the dimension of the network and the number of connected users over the limited shared spectrum, the problems of Inter-User Interference (IUI) become exacerbated. To address these concerns, efficient Multiple Access (MA) technologies, such as Rate-Splitting

Multiple Access (RSMA), have to be utilized [3], [4], [5]. RSMA may be viewed as a generalized Non-Orthogonal Multiple Access (NOMA) and Space-Division Multiple Access (SDMA) framework that is resilient against outdated Channel State Information (CSI) [4], [5].

Given the open nature of the wireless medium, Multi-User (MU) systems are susceptible to especially security breaches, when a massive number of connected users intend to utilize the same spectrum. Traditionally, secure communication is achieved by employing cryptography encryption, which-somewhat optimistically assumes limited computational capabilities for the eavesdroppers (*Eves*), as well as perfectly secure key transfers over the wireless medium. Yet, with the emergence of powerful quantum computers, a persistent and sophisticated *Eve* will be able to extract important confidential information. To circumvent this concern, Physical Layer (PHY)-Security (PLS), which relies on opportunistically exploiting the random nature of the fading channels, has gained significant attention [6], [7], [8]. A pair of potent PLS designs rely on: 1) Optimizing the active transmit precoder (beamformer) of a multi-antenna transmitter, aimed at focusing the transmit power in the directions of legitimate users, while minimizing the energy leakage to *Eves* [9], [10]; 2) intentionally broadcasting specifically designed Artificial Noise (AN) everywhere except for focusing any potential *Eve* [11]. However, both the performance and the design of the aforementioned PLS schemes significantly depends on the accuracy of the knowledge about the *Eve*'s CSI at the legitimate transmitter (E-CSIT) [9], [12].

To meet the demanding KPIs of 6G while securing the confidentiality of the transmitted MUs' messages, RSMA was recently shown to be one of the most effective PLS techniques [12]-[17]. By relying on a secure RSMA Transmit Precoder (TPC) a common message which is constituted by a specific portion of the transmitted message, is introduced at source with a twin-fold mission. More explicitly, apart from serving as the desired message, it also acts as AN without consuming extra power [17]. This is in stark contrast to the conventional AN design, where some portion of the transmit power budget is allocated to AN, hence leading to inefficient usage of the available power budget. Additionally, by optimizing the RSMA TPC at the Base-Station (BS), we can deal with the effects of realistic imperfect channel estimation at the Tx [4], [5], [18]. As a beneficial extension of RS, two-user Cooperative Rate-Splitting (CRS) has been proposed in [19] that outperforms its non-cooperative version [18] in terms of both its reliability [20] and security [12], [16]. Briefly, the CRS framework benefits from the cooperation of the legitimate users, which are allowed to opportunistically forward their

Hamed Bastami and Hamid Behroozi are with the Department of Electrical Engineering, Sharif University of Technology, Tehran, Iran, e-mails: {hamed.bastami@ee., behroozi@}sharif.edu

Majid Moradikia is with Department of Data Science Worcester Polytechnic Institute, Worcester, Massachusetts, e-mail: {mmoradikia@wpi.edu}

Lajos Hanzo is with the University of Southampton, Southampton SO17 1BJ, U.K, e-mail: hanzo@soton.ac.uk.

TABLE I
OVERVIEW OF EXISTING LITERATURE

References⇒ Keywords↓	Proposed Approach	[3]	[4]	[8]	[9]	[10]	[11]	[12]	[13]	[15]	[16]	[17]	[18]	[19]	[22]	[25]	[28]
PLS	✓			✓	✓	✓	✓	✓	✓	✓	✓	✓			✓		✓
Beamformer Design	✓	✓	✓	✓	✓	✓		✓	✓	✓	✓	✓	✓	✓		✓	✓
Unknown Eve						✓											
FJ Design	✓				✓	✓	✓	✓									
SSRM									✓		✓				✓		
UAV-BS	✓	✓					✓	✓	✓			✓			✓	✓	
NOMA		✓								✓			✓			✓	
I-CSIT	✓		✓					✓					✓			✓	
SOPM							✓			✓							
RSMA	✓		✓					✓	✓		✓	✓	✓	✓			✓
CRS	✓							✓	✓		✓			✓			
WCSR	✓		✓					✓				✓					✓
I-ECSIT	✓							✓				✓					✓
SRUS	✓																
MU-CRS	✓																

flawlessly decoded common message to the distant user in two subsequent time-slots.

Recently, Unmanned Aerial Vehicle (UAV)-aided communications have attracted significant research interest [22], [23], [24], thanks to their, on-demand coverage, and the availability of the Line of Sight (LoS) links. In particular, the PLS attained may be readily improved by UAVs upon detecting the *Eve's* location via the UAV-mounted cameras or radar [22]. In practice, only imperfect E-CSIT may be available and thus the conventional PLS schemes no longer perform at their best [12], [17]. Some of the associated challenges have been addressed by the robust PLS solutions designed for UAV-enabled scenarios in [25], [26]. Recently, secure RS and CRS-aided UAV networks relying on realistic imperfect CSIT have been studied respectively in [12], [27]. However, the solutions proposed in [12] and [27] are not applicable for multi-user networks, where secure Relaying Users Selection (SRUS) protocols are necessitated for security reasons. In other words, since all users may act potential candidates for forwarding the common stream during the relaying phase, the question arises: "How to beneficially select the relaying users with the objective of enhancing the security?" None of the above secure UAV-RSMA designs have addressed this important research question. Hence our objective is to close this knowledge gap. Furthermore, to circumvent the deleterious impact of imperfect CSIT, in contrast to [21], we have conceived the worst-case robust designs as well. Explicitly, this is the first work that investigates the robust and secure design of the generalized multi-user C-RSMA downlink of UAV networks. To gain deeper insights, the novelty of the proposed approach is boldly and explicitly contrasted to the state-of-the-art in Table I at a glance. Table II provides a list of acronyms used in this paper.

Against this background, the detailed contributions of our work are summarized as follows:

TABLE II
LIST OF ACRONYMS AND ABBREVIATIONS

PLS	Physical Layer Security
FJ	Friendly Jammer
UAV-BS	Unmanned Aerial Vehicle Base-Station
SIC	Successive Interference Cancellation
I-ESIT	Imperfect <i>Eve's</i> Channel State Information
RSMA	Rate-Splitting Multiple Access
MU-CRS	Multi User Cooperative Rate-Splitting
NRS	Non-Cooperative Rate-Splitting
NOMA	Non-Orthogonal Multiple Access
SDMA	Space Division Multiple Access
EIR	Estimated Information Rates
WCSR	Worst Case Secrecy Rate Maximization
ACC	Actual Channel Capacities
AN	Artificial Noise
CEU	Cell Edge Users
CCU	Cell Center Users
WCSR	Worst-Case Secrecy Rate
IUI	Inter-User Interference
LoS	Line of Sight
MISO-BC	Multi-Input Single-Output Broadcast Channel
TPC	Transmit Precoder
MA	Multiple Access
SPCA	Sequential Parametric Convex Approximation
SURS	Secure Relaying Users Selection

- By relying on the two-stage multi-user C-RSMA philosophy, we follow the secrecy policy of [12] for safeguarding the first cooperative phase through the secure design of the common RSMA TPC. Interestingly, by decoding and forwarding the common stream, two opportunities are provided to take full advantage of the common

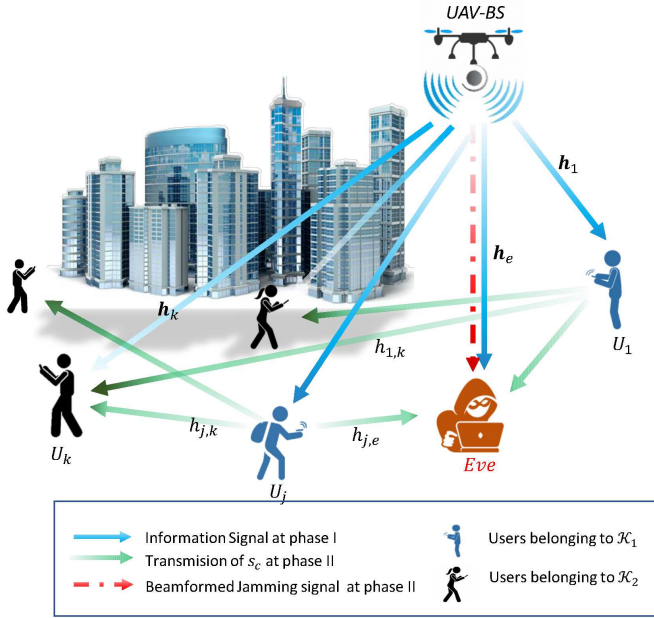


Fig. 1. The proposed cooperative rate-splitting UAV network.

stream, hence further enhancing the secrecy. However, for preventing the interception of the common message during the second phase, the AN is directed towards the *Eve* by designing a robust Maximum Ratio Transmission (MRT) beamformer, which is achieved by harnessing an idle UAV to serve as a jammer during the relaying phase.

- To safeguard confidentiality in the presence of *Eve*, we conceive a generalized multi-user C-RSMA secrecy design, where we optimize the TPCs, the message split, the time slot allocation, the jamming power as well as SRUS to guarantee both secrecy fairness among all users and robustness against imperfect E-CSIT. To satisfy our secrecy fairness objective, we formulate the associated Worst-Case Secrecy Rate (WCSR) maximization problem optimized subject to specific secrecy policy constraints due to the common message rate as well as the power budget constraints imposed on the UAV-BSs during both the transmission and phases.
- To circumvent the discrete nature of the SRUS process as well as the non-convexity of our problem, we propose a two-stage algorithm where SRUS and network parameter optimization is accomplished in two consecutive stages. As for the SRUS, we study both the centralized and distributed protocols. On the other hand, for jointly optimizing the precoders, message split, time slot allocation, and jamming power we resort to the Sequential Parametric Convex Approximation (SPCA) algorithm. This allows us to strike a trade-off between accuracy of approaching the optimal solution and the computational complexity.
- Numerical results show that by applying the proposed solution, the WCSR is substantially boosted over that of the non-cooperative benchmarks over a wide range of network loads.

The rest of this paper is organized as follows. The system

model, signal representation, corresponding achievable information rate and other preliminaries are provided in Section II. Section III formulates our robust WCSR maximization problem and optimal SRUS protocol. The proposed SPCA-based solution, the associated feasible initialization procedures, and our complexity as well as convergence analysis are provided in Section IV. In Section V, our simulation results are presented and conclude in Section VI. Finally, the Appendices and proofs of the lemmas are provided.

Notation: Vectors and matrices are denoted by lower-case and upper-case boldface symbols, respectively; $(\cdot)^T$, $(\cdot)^*$, $(\cdot)^H$, and $(\cdot)^{-1}$ denote the transpose, conjugate, conjugate transpose, and inverse of a matrix respectively; $\Re(\cdot)$ denote the real part of a complex variable, and $\Im(\cdot)$ denote the imaginary part of a complex variable; We use $\mathbb{E}\{\cdot\}$ and \triangleq to denote the expectation and definition operations, respectively; A complex Gaussian random variable with mean μ and variance σ^2 reads as $\mathcal{CN}(\mu, \sigma^2)$; The notation \mathbf{I}_N denotes the $N \times N$ identity matrix; $\mathbb{R}^{N \times 1}$ and $\mathbb{C}^{N \times 1}$ denote the set of N -dimensional standard real and complex Gaussian random variable, respectively; $\mathbb{C}^{N \times N}$ stands for an $N \times N$ element standard complex Gaussian random matrix whose real and imaginary parts are independent normally distributed random variables with mean zero and variance $\frac{1}{2}$; Finally, the entry in the i -th row and j -th column of a matrix \mathbf{H} is represented by $\mathbf{H}[i, j]$.

II. SYSTEM MODEL AND PRELIMINARIES

We commence by introducing the principles of C-RSMA and the channel models. The system model considered is illustrated in Fig. 1, in which a multi-antenna UAV-BS aims for concurrently serving K legitimate users on the ground indexed by the set $\mathcal{K} = \{1, 2, \dots, K\}$ in the presence of an *Eve*, who silently engages in covert wiretapping. While the UAV-BS is equipped with N_t transmit antennas, the terrestrial nodes are assumed to be single-antenna devices. For simultaneously serving multiple users, the UAV-BS is supported by RSMA. Note that, as it will be discussed later in detail, to take full advantage of RSMA, we exploit the more sophisticated C-RSMA technique in this paper, in which two groups of users are considered for each transmission slot. Thus, the users are divided into two different groups: Cell Center Users (CCU) indexed by the set \mathcal{K}_1 , and Cell Edge Users (CEU) indexed by the set \mathcal{K}_2 , so that we have $\mathcal{K}_1 \cup \mathcal{K}_2 = \mathcal{K}$. We assume furthermore that the channel conditions of the users of \mathcal{K}_1 are superior to the channels of those belonging to \mathcal{K}_2 .

A. Principles of C-RSMA

Based on the principle of C-RSMA, the signal transmission is completed in two consecutive phases:

- 1) Broadcasting Phase (BP), where the UAV-BS transmits the RSMA precoded signal towards the terrestrial nodes through the typical Multiple Input Single Output (MISO) Downlink (DL) channels, i.e., represented by $\text{UAV-BS} \rightarrow \{U_k |_{k \in \mathcal{K}}, Eve\}$,
- 2) Relaying Phase (RP), where users within \mathcal{K}_1 , cooperatively forward the signals to CEUs, i.e., $\{U_k |_{k \in \mathcal{K}_1}\} \rightarrow \{U_k |_{k \in \mathcal{K}_2}, Eve\}$.

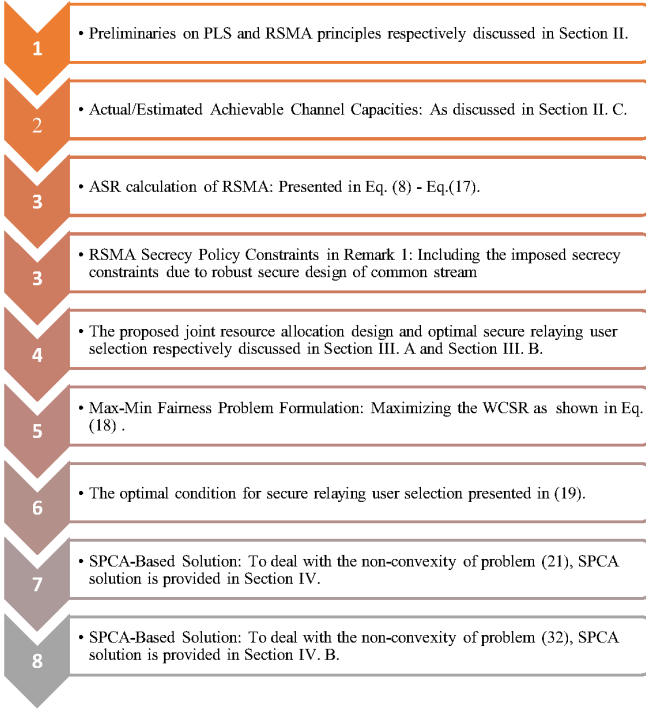


Fig. 2. Flow of the mathematical analysis

The number of time-slots allocated to the two phases may not be equal. Hence, we introduce a dynamic time-slot allocation parameter $0 < \theta \leq 1$, where the fraction θ of time is dedicated for the BP and the remaining portion $(1 - \theta)$ is allocated for the RP.

Following the 1-layer RSMA principle [20], the confidential messages of each legitimate user $\mathcal{W}_k|_{k=1}^K$ are split into the common parts $\mathcal{W}_k^c|_{k=1}^K$ and the private parts $\mathcal{W}_k^p|_{k=1}^K$. The so-obtained common parts are then incorporated into a common codebook for generating the unified common stream s_c . By contrast, $\mathcal{W}_k^p|_{k=1}^K$ are independently encoded into the private streams $s_k|_{k=1}^K$, respectively. If we define $\mathbf{s} \triangleq [s_1, s_2, \dots, s_K]^T$ with a normalized power of $\mathbb{E}\{\mathbf{s}\mathbf{s}^H\} = \mathbf{I}_{K+1}$ and $\mathbf{P} \triangleq [\mathbf{p}_c, \mathbf{p}_1, \dots, \mathbf{p}_K]^T$ as the TPC matrix adopted by the UAV-BS, where \mathbf{p}_c and $\mathbf{p}_k|_{k=1}^K$ respectively stand for the parts corresponding to the common and private streams, then the RSMA DL signal transmitted during the BP is given by:

$$\mathbf{x}^{(1)} = \mathbf{P}\mathbf{s} = \sum_{k \in \mathcal{K}} \mathbf{p}_k s_k + \mathbf{p}_c s_c. \quad (1)$$

At the receiver side, each user first recovers \mathcal{W}_k^c from the detected s_c and then removes the common stream by performing Successive Interference Cancellation (SIC). Then, each user detects its corresponding private stream. By combining \mathcal{W}_k^c with the respective private message, each user can retrieve its original intended message \mathcal{W}_k . During the RP, only the decoded common streams are forwarded to the CEUs. According to the above discussion, two opportunities are provided for *Eve* to infer the information during the two phases of transmissions. To guarantee the security, while each

user is expected to be able to decode s_c , as a part of its original message, the corresponding common TPC, i.e., \mathbf{p}_c , must be designed for ensuring that s_c simultaneously plays the role of undecodable jamming signal at *Eve*. Since the UAV-BS is idle during the RP, we assume that it serves as a friendly jammer during this phase to further enhance the secrecy.

B. Channel Models

We focus on a quasi-static fading environment and denote the channel coefficients of the links spanning from the UAV-BS to terrestrial legitimate nodes and *Eve* respectively by $\mathbf{h}_k \in \mathbb{C}^{N_t \times 1}$ and $\mathbf{h}_e \in \mathbb{C}^{N_t \times 1}$. These channels are modeled as $\mathbf{h}_n \triangleq PL(d_n) \mathbf{n}_n$, $\forall n \in \{\mathcal{K}, e\}$, where $PL(d_n)$ represent the path-loss characterized by the Aerial-to-Ground (A2G) distance d_n , and $\mathbf{n}_n \sim \mathcal{CN}(0, \mathbf{I}_{N_t})$ represents the corresponding small scale fading. Similarly, $h_{j,i} \triangleq PL(d_{j,i}) n_{j,i}$, $\forall j \in \{\mathcal{K}_1\}, \forall i \in \{\mathcal{K}_2, e\}$ stands for the Single Input Single Output (SISO) channel from CCUs and CEUs as well as *Eve* during RP.

Since large-scale fading varies smoothly, we suppose that the UAV-BS can obtain the path-loss variable perfectly for the entire links. Additionally, for the A2G legitimate links $\text{UAV} \rightarrow \{U_k|_{k \in \mathcal{K}_1}\}$, we assume that the small-scale fading component can be obtained accurately by frequently sending handshaking signals. However, concerning the *Eve*, as an untrustworthy subscriber who does not regularly interact with the UAV-BS, its CSI would be outdated at the UAV-BS owing to signaling delays, i.e., Imperfect E-CSIT, although *Eve* might be able to perfectly estimate its corresponding channels in the worst-case secrecy scenario. Thus, for the illegitimate links during both phases $\{\text{UAV}, U_k|_{k \in \mathcal{K}_1}\} \rightarrow \text{Eve}$ we assume that the large-scale fading can be estimated perfectly, and imperfection can only contaminate the small-scale fading component. To characterize the imperfect E-CSIT, we utilize the worst-case model of [28], [29], by which the small-scale fading coefficients of the $\text{UAV} \rightarrow \text{Eve}$ and $\{U_k|_{k \in \mathcal{K}_1}\} \rightarrow \text{Eve}$ channels are formulated as follows:

$$\mathbf{n}_e \triangleq \hat{\mathbf{n}}_e + \Delta \mathbf{n}_e, \quad \Theta_e = \left\{ \Delta \mathbf{n}_e \in \mathbb{C}^{N_t \times 1} : \|\Delta \mathbf{n}_e\|^2 \leq N_t \zeta^2 \right\}, \quad (2)$$

$$n_{j,e} \triangleq \hat{n}_{j,e} + \Delta n_{j,e}, \quad \Theta_{h_{j,e}} = \left\{ \Delta n_{j,e} : |\Delta n_{j,e}|^2 \leq \zeta^2 \right\},$$

$\forall j \in \mathcal{K}_1$, where $\hat{\mathbf{n}}_e$ and $\hat{n}_{j,e}$ are respectively the estimated small-scale fading of *Eve* available for the UAV-BS. Furthermore, $U_j|_{j \in \mathcal{K}_1}$, and $\Delta \mathbf{n}_e$ and $\Delta n_{j,e}$ respectively stand for the unknown channel uncertainty corresponding to \mathbf{n}_e and $n_{j,e}$. Still referring to (2), ζ specifies the radius of the bounded error regions of $\Delta n_{j,e}$, whilst for $\Delta \mathbf{n}_e$ the error is a region bounded with radius $\sqrt{N_t} \zeta$. Specifically, $\zeta > 0$ denotes the size of the uncertainty region of the small-scale fading estimate of the *Eve*. Therefore, the estimated gains of the $\text{UAV} \rightarrow \text{Eve}$ and $U_j|_{j \in \mathcal{K}_1} \rightarrow \text{Eve}$ channel are $\hat{\mathbf{h}}_e = PL(d_e) \hat{\mathbf{n}}_e$ and $\hat{h}_{j,e} = PL(d_{j,e}) \hat{n}_{j,e}$.

C. Performance Metrics and Constraints

In this section, we derive the Achievable Secrecy Rate (ASR) as the objective function considered followed by the

constraints imposed, which must be taken into account in our design. Before proceeding, we have provided a flow-diagram in Fig. 2 to show the flow of the analysis described in the sequel. Again, the worst-case secrecy scenario is considered in this paper, where only imperfect E-CSIT is available at the UAV-BS. Given this perspective, while *Eve* can achieve the actual channel capacity, the UAV-BS is only capable of achieving the estimated information rate. In the following, we derive the Actual Channel Capacities (ACC) as well as the Estimated Information Rates (EIR).

1) *Received Signal Models*: During the BP, the UAV-BS broadcasts the RSMA signal $\mathbf{x}^{(1)}$ and the terrestrial nodes, i.e., $\{U_k|_{k \in \mathcal{K}}\}$ and *Eve*, will respectively receive the following signals:

$$y_k^{(1)} = \mathbf{h}_k^H \mathbf{x}^{(1)} + z_k^{(1)}, \forall k \in \mathcal{K} \quad (3)$$

$$y_e^{(1)} = \mathbf{h}_e^H \mathbf{x}^{(1)} + z_e^{(1)}, \quad (4)$$

where $z_k^{(1)} \sim \mathcal{CN}(0, \sigma_k^2)$ and $z_e^{(1)} \sim \mathcal{CN}(0, \sigma_e^2)$ respectively stand for the Additive White Gaussian Noise (AWGN). During the RP, the j -th CCU re-encodes the s_c and forwards it towards the CEUs at a power of p_j . Concurrently, using the estimated channel $\hat{\mathbf{h}}_e$, the UAV-BS assigns the beamforming vector $\hat{\mathbf{p}}_z \triangleq \frac{\hat{\mathbf{h}}_e^H}{\|\hat{\mathbf{h}}_e\|}$ directed towards the *Eve* with the power of p_z to cover the transmission of s_c against *Eve*. Hence, the signals transmitted during the RP respectively from the UAV-BS and the j -th CCU are given by:

$$x_z^{(2)} = \sqrt{p_z} \hat{\mathbf{p}}_z z, \text{ and } x_j^{(2)} = \sqrt{p_j} s_c \forall j \in \mathcal{K}_1. \quad (5)$$

Subsequently, the signals received by k -th CEU and *Eve* in the RP become:

$$y_k^{(2)} = \sum_{j \in \mathcal{K}_1} h_{j,k}^H x_j^{(2)} + \sqrt{p_z} \mathbf{h}_k^H \hat{\mathbf{p}}_z z + z_k^{(2)}, \forall k \in \mathcal{K}_2 \quad (6)$$

$$y_e^{(2)} = \sum_{j \in \mathcal{K}_1} h_{j,e}^H x_j^{(2)} + \sqrt{p_z} \mathbf{h}_e^H \hat{\mathbf{p}}_z z + z_e^{(2)}, \quad (7)$$

where $z_k^{(2)} \sim \mathcal{CN}(0, \sigma_k^2)$ and $z_e^{(2)} \sim \mathcal{CN}(0, \sigma_e^2)$ are the AWGN at the legitimate user $\{U_k|_{k \in \mathcal{K}_2}\}$ and *Eve*, respectively.

2) *ACC and EIR Analysis*: The CCUs first decode s_c , while treating the signals corresponding to all the private messages as noise. Accordingly, the channel capacities achieved by $\{U_k|_{k \in \mathcal{K}}\}$ and *Eve* in decoding s_c during the BP is given by:

$$R_{c,k}^{(1)} = \theta \log_2 \left(1 + \frac{|\mathbf{h}_k^H \mathbf{p}_c|^2}{\sum_{j \in \mathcal{K}} |\mathbf{h}_k^H \mathbf{p}_j|^2 + \sigma_k^2} \right), \quad (8)$$

$$R_{c,e}^{(1)} = \theta \log_2 \left(1 + \frac{|\mathbf{h}_e^H \mathbf{p}_c|^2}{\sum_{j \in \mathcal{K}} |\mathbf{h}_e^H \mathbf{p}_j|^2 + \sigma_e^2} \right), \quad (9)$$

$\forall k \in \mathcal{K}$. Under the assumption of perfect SIC, the decoded common message is fully eliminated from the received signal and then each user decodes the intended private message by treating the remaining interference inflicted by the other private messages as a noise. Therefore, only the unintended private stream can be considered as interference and the ACC of decoding the private message by $\{U_k|_{k \in \mathcal{K}}\}$ is calculated as:

$$R_{p,k} = \theta \log_2 \left(1 + \frac{|\mathbf{h}_k^H \mathbf{p}_k|^2}{\sum_{j \in \mathcal{K}, j \neq k} |\mathbf{h}_k^H \mathbf{p}_j|^2 + \sigma_k^2} \right), \quad (10)$$

$\forall k \in \mathcal{K}$. Upon using the RSMA technique, an appropriate secrecy policy is to design the common TPC for ensuring that *Eve* is unable to decode s_c . By doing so, s_c can no longer be eliminated through the preceding SIC block and its corresponding term is considered as interference at *Eve*. Thus, considering that *Eve* has a single chance of deciphering the private messages during the first phase, the SINR associated with the detection of the private stream of $U_k|_{k \in \mathcal{K}}$, while treating the private stream of the other users $U_j|_{j \in \mathcal{K}, j \neq k}$ as well as the common stream as interference, may be expressed as:

$$R_{k,e} = \theta \log_2 \left(1 + \frac{|\mathbf{h}_e^H \mathbf{p}_k|^2}{|\mathbf{h}_e^H \mathbf{p}_c|^2 + \sum_{j \in \mathcal{K}, j \neq k} |\mathbf{h}_e^H \mathbf{p}_j|^2 + \sigma_e^2} \right). \quad (11)$$

During the RP, the ACC in decoding the s_c at $U_k|_{k \in \mathcal{K}_2}$ and *Eve* are respectively given by:

$$R_{c,k}^{(2)} = (1 - \theta) \log_2 \left(1 + \frac{\sum_{j \in \mathcal{K}_1} p_j |h_{j,k}|^2}{p_z \|\mathbf{h}_k^H \hat{\mathbf{p}}_z\|^2 + \sigma_k^2} \right), \quad (12)$$

$$R_{c,e}^{(2)} = (1 - \theta) \log_2 \left(1 + \frac{\sum_{j \in \mathcal{K}_1} p_j |h_{j,e}|^2}{p_z \|\mathbf{h}_e^H \hat{\mathbf{p}}_z\|^2 + \sigma_e^2} \right). \quad (13)$$

Notably, the users in \mathcal{K}_2 and *Eve* combine the decoded common message in both phases. However, while the achievable capacity of decoding the common message at all $U_k|_{k \in \mathcal{K}}$ is limited by the worst-case user, i.e., by user receiving at the minimum SINR in detecting s_c during both phases, *Eve* tries to infer s_c up to the sum-capacity of both phases. Accordingly, the achievable rate of decoding s_c at $U_k|_{k \in \mathcal{K}}$ and *Eve* are given as:

$$R_c = \min \left\{ \underbrace{R_{c,k}^{(1)} \Big|_{\forall k \in \mathcal{K}_1}}_{R_{c,\mathcal{K}_1}}, \underbrace{(R_{c,k}^{(1)} + R_{c,k}^{(2)}) \Big|_{\forall k \in \mathcal{K}_2}}_{R_{c,\mathcal{K}_2}} \right\} \\ = \min \{R_{c,\mathcal{K}_1}, R_{c,\mathcal{K}_2}\}. \quad (14)$$

Then, due to the deleterious impact of imperfect E-CSIT, the EIR corresponding to the *Eve*'s link from the UAV-BS

viewpoint is formulated as follows:

$$\hat{R}_{c,e}^{(1)} = \theta \log_2 \left(1 + \frac{|\hat{\mathbf{h}}_e^H \mathbf{p}_c|^2}{\sum_{j \in \mathcal{K}} |\hat{\mathbf{h}}_e^H \mathbf{p}_j|^2 + \sigma_e^2} \right), \quad (15)$$

$$\hat{R}_{c,e}^{(2)} = (1 - \theta) \log_2 \left(1 + \frac{\sum_{j \in \mathcal{K}_1} p_j |\hat{h}_{j,e}|^2}{p_z \|\hat{\mathbf{h}}_e^H \hat{\mathbf{p}}_z\|^2 + \sigma_e^2} \right), \quad (16)$$

$$\hat{R}_{k,e} = \theta \log_2 \left(1 + \frac{|\hat{\mathbf{h}}_e^H \mathbf{p}_k|^2}{|\hat{\mathbf{h}}_e^H \mathbf{p}_c|^2 + \sum_{j \in \mathcal{K}, j \neq k} |\hat{\mathbf{h}}_e^H \mathbf{p}_j|^2 + \sigma_e^2} \right). \quad (17)$$

Remark 1 (Secrecy Policy). To ensure that the common message is decodable for each legitimate user, the actual transmission rate of the common message r_c should satisfy the condition $r_c \leq R_c$. On the other hand, we aim for designing \mathbf{p}_c at the UAV-BS, so that the common message cannot be decoded and plays the role of interference at the *Eve*. For this purpose, we have to satisfy another condition we have to satisfy another condition, namely $r_c > R_{c,e}$. As a result, the corresponding SINR of the private message at the *Eve* is degraded by the interference caused by the undecodable common message.

Remark 2 (Common Message Considerations). R_c is shared among all users to see whether the condition C_1 , pointed out in Remark 1, is satisfied or not. Thus, the rate contributions of each user in transmitting \mathcal{W}_k^c , denoted by \mathcal{C}_k^c , should be tuned at the UAV-BS so that we have $R_c = \sum_{k \in \mathcal{K}} \mathcal{C}_k^c$, where $\mathcal{C}_k^c = x_k R_c$. The weighting factors $x_k \in (0, 1)$ associated with $\sum_{k \in \mathcal{K}} x_k = 1$ enable us to flexibly adjust the significance of each user as part of the common secrecy rate enhancement.

The total achievable secrecy rate of k -th user is given by $\mathcal{R}_k^{\text{sec}} = \mathcal{R}_{k,c}^{\text{sec}} + \mathcal{R}_{k,p}^{\text{sec}}$, where $\mathcal{R}_{k,c}^{\text{sec}} = x_k [R_c - R_{c,e}]^+$ and $\mathcal{R}_{k,p}^{\text{sec}} = [R_{p,k} - R_{k,e}]^+$ represent the achievable secrecy rate of the common message and private message transmitted to the k -th user, respectively.

III. PROPOSED JOINT RESOURCE ALLOCATION AND SRUS

Under the realistic imperfect CSIT assumption, the performance of the MRT beamformer $\hat{\mathbf{p}}_z$ is degraded. To mitigate this deleterious impact and to guarantee a robust design, we will aim for maximizing the minimum ASR over all possible CSI uncertainties. On the other hand, the system's objective is to maximize the minimum ASR among all legitimate users, with the objective of maintaining secrecy fairness.

A. Optimization Problem

Based on the above discussion, the proposed joint resource allocation design comprised of jointly optimizing the TPC, the common message split, the time slot allocation, and SRUS

with the objective of maximizing the minimum ASR among all users subject to a transmit power constraint at the UAV-BS as well as the RSMA secrecy constraints is formulated by:

$$\max_{\mathbf{P}, \theta, \chi, \mathcal{K}_1, \{p_j\}_{j \in \mathcal{K}_1}, p_z} \left(\min_{k \in \mathcal{K}} \left(\min_{\Delta \mathbf{n}_e, \{\Delta n_{j,e}\}_{j \in \mathcal{K}_1}} \{\mathcal{R}_k^{\text{sec}}\} \right) \right) \quad (18)$$

s.t.

$$\begin{aligned} C_1 &: r_c \leq R_c, \\ C_2 &: R_c = \min \{R_{c,\mathcal{K}_1}, R_{c,\mathcal{K}_2}\}, \\ C_3 &: r_c \geq \max_{\Delta \mathbf{n}_e, \{\Delta n_{j,e}\}_{j \in \mathcal{K}_1}} R_{c,e}, \\ C_4 &: \text{Tr}(\mathbf{P}\mathbf{P}^H) \leq P_t, \\ C_5 &: 0 \leq p_z \leq \bar{P}_z \\ C_6 &: 0 \leq p_j \leq \bar{P}_j \quad \forall j \in \mathcal{K}_1 \\ C_7 &: C_k \geq 0, \quad \forall k \in \mathcal{K} \\ C_8 &: \mathcal{K}_1 \subset \mathcal{K}, \mathcal{K}_2 = \mathcal{K} \setminus \mathcal{K}_1 \\ C_9 &: 0 < \theta \leq 1, \end{aligned}$$

where $\chi \triangleq [x_1, \dots, x_K]$, and P_t stands for the transmit power budget at the UAV-BS. Note that, once \mathcal{K}_1 is determined by solving the optimization problem, $\mathcal{K}_2 \triangleq \mathcal{K} \setminus \mathcal{K}_1$ also becomes specified, and thus only \mathcal{K}_1 is considered as an optimization variable. The problem formulated is a mixed integer non-convex problem due to the discontinuous nature of the variable \mathcal{K}_1 . The optimal SRUS problem itself imposes high computational complexity and the resultant cost increases upon growing the number of users. To circumvent this difficulty, we propose a low-cost algorithm including the following two main steps. Firstly, SRUS protocol is performed to find optimum \mathcal{K}_1^* and \mathcal{K}_2^* . In the next step, based on the \mathcal{K}_1^* and \mathcal{K}_2^* we jointly optimize the other network parameters.

B. Optimal SRUS

The SRUS protocol must address two questions:

- How do we select the relaying users?
- How many relaying users are needed?

In order to address these research questions, we turn to the following proposition.

Proposition 3. *At the global by optimal point $(\mathbf{P}^*, \theta^*, \chi^*, \mathcal{K}_1^*, \{p_j^*\}_{j \in \mathcal{K}_1^*}, p_z^*)$ of problem (18), the common secrecy rates achieved by the users in the set \mathcal{K}_1^* , i.e., $\mathcal{R}_{c,\mathcal{K}_1^*}^{\text{sec}}$, and set \mathcal{K}_2^* , i.e., $\mathcal{R}_{c,\mathcal{K}_2^*}^{\text{sec}}$, are equal which can be formulated as:*

$$\underbrace{\min_{k \in \mathcal{K}_1^*} \{\mathcal{R}_{c,k}^{\text{sec}(1)}\}}_{\mathcal{R}_{c,\mathcal{K}_1^*}^{\text{sec}}} = \underbrace{\min_{k \in \mathcal{K}_2^*} \{\mathcal{R}_{c,k}^{\text{sec}(1)} + \mathcal{R}_{c,k}^{\text{sec}(2)}\}}_{\mathcal{R}_{c,\mathcal{K}_2^*}^{\text{sec}}}, \quad (19)$$

Proof: See Appendix A. ■

Remark 4. It can be readily concluded from Proposition 3 that the optimal secure relaying user grouping obeys the following rule, when $0 < \theta^* < 1$:

$$\min_{k \in \mathcal{K}_1^*} \{\mathcal{R}_{c,k}^{\text{sec}(1)}\} > \min_{k \in \mathcal{K}_2^*} \{\mathcal{R}_{c,k}^{\text{sec}(2)}\}. \quad (20)$$

$$\min_{k \in \mathcal{K}_1^*} \{R_{c,k}^{(1)}\} > \min_{k \in \mathcal{K}_2^*} \{R_{c,k}^{(1)}\}. \quad (21)$$

Given the insight inferred from Proposition 3, to enhance the common secrecy rate, the users having larger $\mathcal{R}_{c,k}^{\text{sec}(1)}$ in BP and smaller RP leakage tend to be clustered in \mathcal{K}_1 , while the users with lower $\mathcal{R}_{c,k}^{\text{sec}(1)}$ in BP and larger RP leakage tend to fall into \mathcal{K}_2 . Since the $\mathcal{R}_{c,k}^{\text{sec}(1)}$ and RP leakage respectively depends on $\|\mathbf{h}_k\|_2$ and $|\hat{h}_{k,e}|$, an intuitive and simple selection algorithm is based on the simple metric $\frac{\|\mathbf{h}_k\|_2}{|\hat{h}_{k,e}|}$. In the following a pair of relaying protocols (centralized and distributed) based on this metric are presented.

- **Centralized relaying protocol:** Since the UAV-BS needs all the CSIs for its TPC design, one option is to perform SRUS by the UAV-BS. The proposed centralized SRUS algorithm is presented in Algorithm 1, where the process of channel estimation is performed through the classic Request-To-Send (RTS)/Clear-To-Send (CTS) collision avoidance mechanism.
- **Distributed relaying protocol:** In the above centralized protocol, the RTS packet is transmitted through a common downlink pilot channel, while the CTS packets are fed back through individual uplink pilot channels dedicated to each user. Because of this difference between the uplink and downlink centralized techniques are more susceptible to channel imperfections and thus, distributed selection is preferred. More explicitly, while the centralized protocol needs the CSIT for all users at the UAV-BS to select the best secure relaying users, the distributed protocol allows users to select their secure relaying partners based on the CSI estimated at the Receiver (CSIR). This may be readily obtained from the common downlink pilot channels. The proposed distributed SRUS algorithm is presented in Algorithm 2.

IV. NETWORK PARAMETER OPTIMIZATION

Algorithm 1 Centralized SRUS Protocol

Initialization $n = 0, \mathcal{K}_1 = \emptyset$, and $\mathcal{K}_2 = \mathcal{K}$.

Step 1 Channel estimation of Users at UAV-BS: First UAV-BS inform all users about $|\mathcal{K}_1| = K_1$ through a RTS packet and then they respond through a CTS packet by which their channel is estimated at UAV-BS.

Step 2 Ordering the users based on the channel strength $\frac{\|\mathbf{h}_k\|_2}{|\hat{h}_{k,e}|}$.

Step 3 UAV-BS finds \mathcal{K}_1 secure relaying user as follows.

Repeat:

- ① $k^* = \max_k \left\{ \frac{\|\mathbf{h}_k\|_2}{|\hat{h}_{k,e}|} \right\}$
- ② $\mathcal{K}_1 \leftarrow \mathcal{K}_1 \cup \{k^*\}$
- ③ $\mathcal{K}_2 \leftarrow \mathcal{K}_2 \setminus \{k^*\}$

Until $|\mathcal{K}_1| = K_1$.

Output: UAV-BS transmits a "flag" packet containing the selection results to all users.

After relaxing the problem from the discontinuous variables \mathcal{K}_1^* and \mathcal{K}_2^* , in this stage, we aim for optimizing the remaining variables comprised in the set $\{\mathbf{P}, \theta, \chi, \{p_j\}_{j \in \mathcal{K}_1}, p_z\}$.

Algorithm 2 Decentralized SRUS Protocol

Initialization $n = 0, \mathcal{K}_1 = \emptyset$, and $\mathcal{K}_2 = \mathcal{K}$.

Step 1 UAV-BS broadcasts the $|\hat{h}_{k,e}|$ and RTS packet that contains the value of $|\mathcal{K}_1| = K_1$ to all users. Each user receives them, replies to UAV-BS with CTS and estimates the channel \mathbf{h}_k and calculates the $\frac{\|\mathbf{h}_k\|_2}{|\hat{h}_{k,e}|}$.

Step 2 Decentralized SRUS:

Repeat:

- ① At each user in \mathcal{K}_2 , clear the existing timer if it has one.
- ② The timer is reset at each user in \mathcal{K}_2 as $t_k = \frac{1}{\|\mathbf{h}_k\|_2}$, $\forall k \in \mathcal{K}_2$.
- ③ The user who counts down to zero announces himself as the best secure relaying user in \mathcal{K}_2 with a "flag" packet.
- ④ Upon receiving the "flag" packet from the best secure relaying user k^* , each user in \mathcal{K}_2 updates itself as $\mathcal{K}_1 \leftarrow \mathcal{K}_1 \cup \{k^*\}$, $\mathcal{K}_2 \leftarrow \mathcal{K}_2 \setminus \{k^*\}$.

Until $|\mathcal{K}_1| = K_1$.

However, the resultant problem is still non-convex because of the non-convex Objective Function (OF) as well as non-convex constraint set, and thus finding the global optimum is intractable. To circumvent the non-convexity, we design a sub-optimal algorithm relying on the classic SPCA [39]. Using SPCA, the problem is iteratively approximated by a sequence of programs. To facilitate the design of SPCA, we first introduce the auxiliary variable r_{sec} and recast problem (18) into its equivalent epigraph form, given by:

$$\max_{\mathbf{P}, \theta, \chi, \mathcal{K}_1, \{p_j\}_{j \in \mathcal{K}_1}, p_z} r_{sec} \quad (22)$$

s.t.

$$C_1 : \chi_k [R_c - R_{c,e}]^+ + [R_{p,k} - R_{k,e}]^+ \geq r_{sec},$$

$$\forall k \in \mathcal{K}, \forall \Delta \mathbf{n}_e \in \Theta_e, \forall \{\Delta n_{j,e}\}_{j \in \mathcal{K}_1} \in \Theta_{h_{j,e}}$$

$$((18) - C_1), ((18) - C_2), ((18) - C_3), ((18) - C_4), ((18) - C_5),$$

$$((18) - C_6), ((18) - C_7).$$

It is easy to show that (18) and (22) are equivalent, because, upon observing (22), it can be noted that r_{sec} plays the role of lower bound for $\max_{\Delta \mathbf{n}_e, \{\Delta n_{j,e}\}_{j \in \mathcal{K}_1}} \mathcal{R}_k^{\text{sec}}$ in the OF of (18) and its maximization will increase the left-side of the constraints (22 - C₁), so that it would be active at the optimum. After this transformation, the problem (22) is still non- due to the constraints ((18)-C₁)-((18)-C₃). In order to facilitate the procedure of convexifying (22), we further define new sets of auxiliary variables $\beta_p = [\beta_{p,k}]_{\forall k \in \mathcal{K}}$, $\beta_c^{(1)} = [\beta_{c,k}^{(1)}]_{\forall k \in \mathcal{K}}$, $\beta_c^{(2)} = [\beta_{c,k}^{(2)}]_{\forall k \in \mathcal{K}_2}$, $\beta_e = [\beta_{k,e}]_{\forall k \in \mathcal{K}}$, $\alpha_{c,e}$, $\rho_c^{(1)} = [\rho_{c,k}^{(1)}]_{\forall k \in \mathcal{K}}$, $\rho_c^{(2)} = [\rho_{c,k}^{(2)}]_{\forall k \in \mathcal{K}_2}$, and $\rho_p = [\rho_{p,k}]_{\forall k \in \mathcal{K}}$. β_p , β_c , are adopted respectively for representing the rate vectors of the private streams and the common streams (without θ) at all users, while $\alpha_{c,e}$ and β_e represent the rate of the common streams and private streams at Eve, respectively. Finally, ρ_c and ρ_p respectively denote the SINR vectors of the private streams and the common streams at all the users. This allows

us to reformulate (22) into:

$$\max_{\mathbf{P}, \theta, \boldsymbol{\chi}, \mathcal{K}_1, \{p_j\}_{j \in \mathcal{K}_1}, p_z, \boldsymbol{\beta}_{\{c,e,p\}}, \boldsymbol{\rho}_{\{c,p\}}, \alpha_{c,e}} r_{sec} \quad (23)$$

s.t.

$$C_1 : x_k (R_c - \alpha_{c,e}) + \theta (\alpha_{p,k} - \alpha_{e,k}) \geq r_{sec}, \quad \forall k \in \mathcal{K}$$

$$C_2 : \theta \alpha_{c,j} \geq R_c, \quad \forall j \in \mathcal{K}_1$$

$$C_3 : \theta \alpha_{c,k} + R_{c,k}^{(2)} \geq R_c, \quad \forall k \in \mathcal{K}_2$$

$$C_4 : \frac{|\mathbf{h}_k^H \mathbf{p}_k|^2}{\sum_{j \in \mathcal{K}, j \neq k} |\mathbf{h}_k^H \mathbf{p}_j|^2 + \sigma_k^2} \geq \rho_{p,k}, \quad \forall k \in \mathcal{K}$$

$$C_5 : \frac{|\mathbf{h}_k^H \mathbf{p}_c|^2}{\sum_{j \in \mathcal{K}} |\mathbf{h}_k^H \mathbf{p}_j|^2 + \sigma_k^2} \geq \rho_{c,k}^{(1)}, \quad \forall k \in \mathcal{K}$$

$$C_6 : 1 + \rho_{c,k}^{(1)} - 2\beta_{c,k}^{(1)} \geq 0, \quad \forall k \in \mathcal{K}$$

$$C_7 : 1 + \rho_{p,k} - 2\beta_{p,k} \geq 0, \quad \forall k \in \mathcal{K}$$

$$C_8 : R_c \geq r_c,$$

$$C_9 : R_c \geq \alpha_{c,e}, \quad \beta_{p,k} \geq \beta_{k,e}, \quad \forall k \in \mathcal{K}$$

$$C_{10} : r_c \geq \max_{\Delta \mathbf{n}_e, \{\Delta n_{j,e}\}_{j \in \mathcal{K}_1}} R_{c,e},$$

$$C_{11} : \alpha_{c,e} \geq \max_{\Delta \mathbf{n}_e, \{\Delta n_{j,e}\}_{j \in \mathcal{K}_1}} R_{c,e}$$

$$C_{12} : \alpha_{k,e} \geq \max_{\Delta \mathbf{n}_e} R_{k,e}, \quad \alpha_{k,e} \geq \theta \beta_{k,e}$$

$$C_{13} : \sum_{k \in \mathcal{K}} x_k = 1, 0 \leq x_k \leq 1, \quad \forall k \in \mathcal{K}.$$

Despite this linearization, by invoking the definitions of rates, the constraints (23- C_1 : C_5) and (23- C_{10} : C_{12}) are still non-convex. To handle the non-convexity of these constraints we construct a suitable convex inner subset for approximating the non-convex feasible solution set. Given this perspective, we first try to circumvent the bilinear factor $\theta \beta_{p,k}$ that appeared in (23- C_1 : C_3) which can be equivalently reformulated with the aim of linearization as $\theta \beta_{p,k} = \frac{1}{4} (\theta + \beta_{p,k})^2 - \frac{1}{4} (\theta - \beta_{p,k})^2$. Using its first-order Taylor expansion counterpart, at the m -th iteration, $\theta \beta_{p,k}$ is approximated at the point $(\theta^{[m]}, \beta_{p,k}^{[m]})$ as follows:

$$\theta \beta_{p,k} \geq \Theta^{[m]}(\theta, \beta_{p,k}), \quad (24)$$

$$\Theta^{[m]}(\theta, \beta_{p,k}) \triangleq \frac{1}{2} (\theta^{[m]} + \beta_{p,k}^{[m]}) (\theta + \beta_{p,k}) - \frac{1}{4} (\theta^{[m]} + \beta_{p,k}^{[m]})^2 - \frac{1}{4} (\theta - \beta_{p,k})^2.$$

Similarly, to acquire the lower bound of $\theta \beta_{k,e}$, we approximate the term $(\theta - \beta_{k,e})^2$, which appeared in its expanded form, around $(\theta^{[m]}, \beta_{k,e}^{[m]})$ as follows:

$$\theta \beta_{k,e} \leq \bar{\Theta}^{[m]}(\theta, \beta_{k,e}), \quad (25)$$

$$\bar{\Theta}^{[m]}(\theta, \beta_{k,e}) \triangleq \frac{1}{4} (\theta + \beta_{k,e})^2 + \frac{1}{4} (\theta^{[m]} - \beta_{k,e}^{[m]})^2 - \frac{1}{2} (\theta^{[m]} - \beta_{k,e}^{[m]}) (\theta - \beta_{k,e}).$$

By substituting the affine approximation terms obtained in (24) and (25), the constraints (23- C_1 : C_3) around the point $(\theta^{[m]}, \beta_{p,k}^{[m]}, \beta_{k,e}^{[m]}, \beta_{c,j}^{(1)[m]})$ are approximated as follows:

$$C_k - \alpha_{c,e} + \Theta^{[m]}(\theta, \beta_{p,k}) - \bar{\Theta}^{[m]}(\theta, \beta_{k,e}) \geq r_{sec}, \quad \forall k \in \mathcal{K}, \quad (26)$$

$$\Theta^{[m]}(\theta, \beta_{c,k}^{(1)}) \geq \sum_{\forall k' \in \mathcal{K}} C_{k'}, \quad \forall k \in \mathcal{K}_1, \quad (27)$$

$$\Theta^{[m]}(\theta, \beta_{c,k}^{(1)}) + R_{c,k}^{(2)} \geq \sum_{\forall k' \in \mathcal{K}} C_{k'}, \quad \forall k \in \mathcal{K}_2. \quad (28)$$

As for the constraints (23- C_4 : C_5), they can be equivalently expressed through the Difference-of-Convex (DC) decomposition [37], given by:

$$\sum_{j \in \mathcal{K}, j \neq k} |\mathbf{h}_k^H \mathbf{p}_j|^2 + \sigma_k^2 - \underbrace{\frac{|\mathbf{h}_k^H \mathbf{p}_k|^2}{\rho_{p,k}}}_{\mathcal{B}_{p,k}} \leq 0, \quad \forall k \in \mathcal{K} \quad (29)$$

$$\sum_{j \in \mathcal{K}} |\mathbf{h}_k^H \mathbf{p}_j|^2 + \sigma_k^2 - \underbrace{\frac{|\mathbf{h}_k^H \mathbf{p}_c|^2}{\rho_{c,k}^{(1)}}}_{\mathcal{C}_{p,k}} \leq 0, \quad \forall k \in \mathcal{K}. \quad (30)$$

As it can be observed, the non-convexities of (29) and (30) are caused by the concave terms $\mathcal{B}_{p,k}$ and $\mathcal{C}_{p,k}$. Therefore, we replace them by their affine approximation counterparts obtained by the first-order Taylor expansion around the point $(\mathbf{p}_c^{[m]}, \mathbf{p}_k^{[m]}, \rho_{c,k}^{(1)[m]}, \rho_{p,k}^{[m]})$ and obtain the convex approximations of (29) and (30) as follows:

$$\sum_{j \in \mathcal{K}, j \neq k} |\mathbf{h}_k^H \mathbf{p}_j|^2 + \sigma_k^2 - \Psi^{[m]}(\mathbf{p}_k, \rho_{p,k}; \mathbf{h}_k) \leq 0, \quad \forall k \in \mathcal{K} \quad (31)$$

$$\sum_{j \in \mathcal{K}} |\mathbf{h}_k^H \mathbf{p}_j|^2 + \sigma_k^2 - \Psi^{[m]}(\mathbf{p}_c, \rho_{c,k}^{(1)}; \mathbf{h}_k) \leq 0, \quad \forall k \in \mathcal{K} \quad (32)$$

where

$$\Psi^{[m]}(\mathbf{u}, x; \mathbf{h}) \triangleq \frac{2\Re\{(\mathbf{u}^{[m]})^H \mathbf{h} \mathbf{h}^H \mathbf{u}\}}{x^{[m]}} - \frac{|\mathbf{h}^H \mathbf{u}^{[m]}|^2 x}{(x^{[m]})^2}. \quad (33)$$

Now, with the objective of convexifying (23- C_{10} : C_{11}), we can equivalently write them as follows:

$$r_c \geq \alpha_{c,e}, \quad (34)$$

$$\alpha_{c,e} \geq R_{c,e}, \quad \forall \Delta \mathbf{n}_e \in \Theta_e, \quad \forall \{\Delta n_{j,e} \in \Theta_{h_{j,e}}\}_{j \in \mathcal{K}_1}. \quad (35)$$

However, (35) is still non-convex, which enforces us to introduce the new auxiliary variables $\{\rho_{c,e}^{(1)}, \rho_{c,e}^{(2)}, \beta_{c,e}^{(1)}, \beta_{c,e}^{(2)}\}$ representing the SINR, as well as the rate of the common streams associated with first and second phases at Eve, respectively. After some routine mathematical manipulations, (35) can be recast as:

$$\bar{\Theta}^{[m]}(\theta, \beta_{c,e}^{(1)}) + \bar{\Theta}^{[m]}(1 - \theta, \beta_{c,e}^{(2)}) \leq \alpha_{c,e}, \quad (36)$$

$$1 + \rho_{c,e}^{(j)} - \Gamma^{[m]}(\beta_{c,e}^{(j)}) \leq 0, \quad j \in \{1, 2\}, \quad (37)$$

$$\frac{|\mathbf{h}_e^H \mathbf{p}_c|^2}{\sum_{k \in \mathcal{K}} |\mathbf{h}_e^H \mathbf{p}_k|^2 + \sigma_e^2} \leq \rho_{c,e}^{(1)}, \quad \forall \Delta \mathbf{n}_e \in \Theta_e, \quad (38)$$

$$\frac{\sum_{j \in \mathcal{K}_1} p_j |h_{j,e}|^2}{p_z \left\| \mathbf{h}_e^H \hat{\mathbf{p}}_z \right\|^2 + \sigma_e^2} \leq \rho_{c,e}^{(2)}, \quad \forall \Delta \mathbf{n}_e \in \Theta_e, \forall \{\Delta n_{j,e} \in \Theta_{h_{j,e}}\}, \quad (39)$$

where $\Gamma^{[m]}(x) \triangleq 2^{x^{[m]}} [1 + \ln(2)(x - x^{[m]})]$. Here, (38) and (39) are still non-convex, which enforces us to define the new auxiliary variables $\{x_{c,e}, \{u_{k,c,e}\}_{k \in \mathcal{K}}, \{y_{j,c,e}\}_{j \in \mathcal{K}_1}, v_{c,e}\}$, by which we can reformulate (38) and (39) as follows:

$$\frac{x_{c,e}^2}{\sum_{k \in \mathcal{K}} u_{k,c,e} + \sigma_e^2} \leq \rho_{c,e}^{(1)}, \quad (40)$$

$$\frac{\sum_{j \in \mathcal{K}_1} y_{j,c,e}^2}{v_{c,e} + \sigma_e^2} \leq \rho_{c,e}^{(2)}, \quad (41)$$

$$\max_{\forall \Delta \mathbf{n}_e \in \Theta_e} \left| \left(\hat{\mathbf{h}}_e + \Delta \mathbf{n}_e \right)^H \mathbf{p}_c \right| \leq x_{c,e}, \quad (42)$$

$$\min_{\forall \Delta \mathbf{n}_e \in \Theta_e} \left| \left(\hat{\mathbf{h}}_e + \Delta \mathbf{n}_e \right)^H \mathbf{p}_k \right|^2 \geq u_{k,c,e}, \quad \forall k \in \mathcal{K}, \quad (43)$$

$$\max_{\Delta n_{j,e} \in \Theta_{h_{j,e}}} \delta_j \left| \hat{h}_{j,e} + \Delta n_{j,e} \right| \leq y_{j,c,e}, \quad \forall j \in \mathcal{K}_1, \quad (44)$$

$$\min_{\forall \Delta \mathbf{n}_e \in \Theta_e} p_z \left| \left(\hat{\mathbf{h}}_e + \Delta \mathbf{n}_e \right)^H \hat{\mathbf{p}}_z \right|^2 \geq v_{c,e}, \quad (45)$$

where $\delta_j \triangleq \sqrt{p_j}$. Next, we adopt the SPCA method to convert the non-convex constraints (40)-(41) into convex constraints. In this regard, we introduce the auxiliary variables $\{d_{c,e}^{(1)}, d_{c,e}^{(2)}\}$ into the constraints (40)-(41), leading to:

$$\sum_{k \in \mathcal{K}} u_{k,c,e} + \sigma_e^2 \geq d_{c,e}^{(1)}, \quad (46)$$

$$\frac{x_{c,e}^2}{d_{c,e}^{(1)}} \leq \rho_{c,e}^{(1)}, \quad (47)$$

$$v_{c,e} + \sigma_e^2 \geq d_{c,e}^{(2)}, \quad (48)$$

$$\frac{\sum_{j \in \mathcal{K}_1} y_{j,c,e}^2}{d_{c,e}^{(2)}} \leq \rho_{c,e}^{(2)}. \quad (49)$$

Based on the above approximation methods, the original optimization problem can be solved using the SPCA method. The main idea of SPCA is to successively solve a sequence of convex sub-problems. At the m -th iteration, based on the optimal solution $\left(\mathbf{P}^{[m]}, \theta^{[m]}, \boldsymbol{\chi}^{[m]}, \{p_j^{[m]}\}_{j \in \mathcal{K}_1}, p_z^{[m]}, \boldsymbol{\beta}_{\{c,e,p\}}^{[m]}, \boldsymbol{\rho}_{\{c,p\}}^{[m]}, \alpha_{c,e}^{[m]} \right)$ obtained from the previous $(m-1)$ -st iteration, we solve the following sub-problem:

$$\max_{\mathbf{P}, \theta, \boldsymbol{\chi}, \mathcal{K}_1, \{p_j\}_{j \in \mathcal{K}_1}, p_z, \boldsymbol{\beta}_{\{c,e,p\}}, \boldsymbol{\rho}_{\{c,p\}}, \alpha_{c,e}} r_{\text{sec}}^{[m]} \quad (50)$$

s.t. (24)-(28), (32), (33), (37), (38), (47)-(52), 23-C13, (23 -C4 : C7), (18 -C4 : C7).

Using the interior-point methods of [37], we can solve the problem in (20), which is a convex Quadratically Constrained Quadratic Program (QCQP) [37].

A. Feasible Initial Point Search Algorithm

Note that, if (50) is initialized by random points, it may fail at the very beginning, because of infeasibility [1], [5], [10]. To circumvent this issue, we now conceive a feasible initial point search algorithm (FIPSA) in this section. In this regard, we aim for minimizing an infeasibility indicator parameter $\vartheta > 0$, to flag up any violation of the constraints of (50). Hence we have to rewrite all the constraints of problem (50) in the form of $\mathcal{G}_i(\mathbf{x})|_{i=1}^{16} \leq \vartheta$, where $\mathbf{x} \triangleq \left(\mathbf{P}, \theta, \boldsymbol{\chi}, \mathcal{K}_1, \{p_j\}_{j \in \mathcal{K}_1}, p_z, \boldsymbol{\beta}_{\{c,e,p\}}, \boldsymbol{\rho}_{\{c,p\}}, \alpha_{c,e} \right)$ and $\mathcal{G}_i(\mathbf{x})$ stands for the reshaped format of the i -th constraint and all the terms at the left-side of the less than or equal to zero. Then we reformulate the feasibility problem as follows:

$$\min_{\mathbf{x}} \vartheta \quad (51)$$

s.t. $\mathcal{G}_i(\mathbf{x})|_{i=1}^{16} \leq \vartheta$.

This approach has been previously proposed in [9], [12] as a low-complexity technique of finding feasible initial points. Overall, the proposed FIPSA runs at the first step and then the initial points (IP)s calculated are fed to (50). As a starting point, FIPSA commences with following IPs and the algorithm is halted if either the stopping criterion is satisfied or the maximum number of affordable iterations is reached. In this regard, the TPCs of the proposed FIPSA algorithm are initialized by using MRT combined with Singular Value Decomposition (SVD). The TPC $\{\mathbf{p}_k^{[0]}\}_{k \in \mathcal{K}}$ constructed for

the private stream $\{s_k\}_{k \in \mathcal{K}}$ is initialized as $\sqrt{\omega} \frac{P_t}{K} \frac{\mathbf{h}_k}{\|\mathbf{h}_k\|}$, where $0 < \omega < 1$. The TPC $\mathbf{p}_c^{[0]}$ for the common message s_c is initialized as $\sqrt{(1-\omega)} P_t \mathbf{u}_c$, and \mathbf{u}_c is the largest left singular vector of the channel matrix $\mathbf{A} \triangleq [\mathbf{h}_1, \mathbf{h}_2, \dots, \mathbf{h}_K]$. It is calculated by $\mathbf{u}_c \triangleq \mathbf{U}_c(:, 1)$ where $\mathbf{A} \triangleq \mathbf{USD}^H$. Also we have initialized the iterative variables as $\theta^{[0]} = 0.5$, $p_z^{[0]} = \omega_z \bar{P}_z$, $p_j^{[0]} = \omega_j \bar{P}_j$ where $0 < \{\omega_j, \omega_z\} < 1$,

$$\rho_{c,k}^{(1)[0]} = \frac{|\mathbf{h}_k^H \mathbf{p}_c^{[0]}|^2}{\sum_{j \in \mathcal{K}} |\mathbf{h}_k^H \mathbf{p}_j^{[0]}|^2 + \sigma_k^2}, \quad \rho_{c,k}^{(2)[0]} = \frac{\sum_{j \in \mathcal{K}_1} p_j^{[0]} |h_{j,k}|^2}{p_z^{[0]} \|\mathbf{h}_k^H \hat{\mathbf{p}}_z\|^2 + \sigma_k^2},$$

$$\rho_{c,e}^{(1)[0]} = \frac{|\mathbf{h}_e^H \mathbf{p}_c^{[0]}|^2}{\sum_{j \in \mathcal{K}} |\mathbf{h}_e^H \mathbf{p}_j^{[0]}|^2 + \sigma_e^2}, \quad \rho_{c,e}^{(2)[0]} = \frac{\sum_{j \in \mathcal{K}_1} p_j^{[0]} |h_{j,e}|^2}{p_z^{[0]} \|\mathbf{h}_e^H \hat{\mathbf{p}}_z\|^2 + \sigma_e^2},$$

$$\rho_{p,k}^{[0]} = \frac{|\mathbf{h}_k^H \mathbf{p}_k^{[0]}|^2}{\sum_{j \in \mathcal{K}, j \neq k} |\mathbf{h}_k^H \mathbf{p}_j^{[0]}|^2 + \sigma_k^2}, \quad \rho_{k,e}^{[0]} = \frac{|\mathbf{h}_e^H \mathbf{p}_k^{[0]}|^2}{\sum_{j \in \mathcal{K}, j \neq k} |\mathbf{h}_e^H \mathbf{p}_j^{[0]}|^2 + \sigma_k^2},$$

$$\beta_{c,k}^{(n)[0]} = \log_2 \left(1 + \rho_{c,k}^{(n)[0]} \right), \quad \beta_{c,e}^{(n)[0]} = \log_2 \left(1 + \rho_{c,e}^{(n)[0]} \right)$$

$$\forall n \in \{1, 2\}, \quad \beta_{p,k}^{[0]} = \log_2 \left(1 + \rho_{p,k}^{[0]} \right), \quad \beta_{k,e}^{[0]} =$$

$$\log_2 \left(1 + \rho_{k,e}^{[0]} \right), \quad \alpha_{c,e}^{[0]} = \theta^{[0]} \beta_{c,e}^{(1)[0]} + (1 - \theta^{[0]}) \beta_{c,e}^{(2)[0]}, \quad R_c^{[0]} =$$

$$\min \left\{ \left\{ \theta^{[0]} \beta_{c,j}^{(1)[0]} \right\}_{j \in \mathcal{K}_1}, \left\{ \theta^{[0]} \beta_{c,k}^{(1)[0]} + (1 - \theta^{[0]}) \beta_{c,k}^{(2)[0]} \right\}_{k \in \mathcal{K}_2} \right\}$$

and $\chi_k^{[0]} = \frac{1}{R_k}$.

B. Convergence Analysis

The proposed SPCA-based algorithm iteratively solves the approximated problem (23) until convergence is reached, where δ represents the convergence tolerance. In this regard, we formulate the following proposition.

Proposition 5. *The proposed SPCA-based algorithm guarantees convergence to a stationary point of problem (22) for any feasible initial point.*

Proof: See Appendix B. ■

C. Complexity Analysis

The SPCA-based solution suggested solves the convex subproblem (50) in each iteration. Problem (50) is a generalized nonlinear convex program due to the exponential cone constraints ($23-C_6 : C_7$). In order to approximate ($23-C_6 : C_7$), a sequence of Second Order Cones (SOCs) would be more efficient [38]. Hence, we can use one of the MATLAB optimization Toolbox solvers, such as *cvx* or *fmincon*. Considering the computational complexity of interior-point methods, i.e., $\mathcal{O}([KN_t]^{3.5})$, it is possible to solve the resultant SOC program. The total number of iterations required for achieving convergence may be shown to be on the order of $\mathcal{O}(-\log(\zeta))$. Therefore, the worst-case computational complexity is $\mathcal{O}(-\log(\delta) \times [KN_t]^{3.5})$.

V. NUMERICAL RESULTS

In this section, we present numerical results for characterizing our proposed framework using the following simulation setting, unless stated otherwise. The simulation results are averaged over 10^2 random realizations of the proposed scheme. Through this section, a maximum of 25 iterations are considered for our proposed secrecy fairness maximization problem to converge. Moreover, we set the maximum convergence tolerance to be $\delta = 10^{-2}$. In contrast to the fading model between users, the path loss model of our UAV network includes both LoS and NLoS in conjunction with the path-loss exponents $\mathcal{L}_{n,k}^i = 2$ and $\mathcal{N}_{n,k}^i = 3.5$, respectively. We assume that the transmit power obeys $\bar{P}_j = \bar{P}_z = \frac{P_t}{2}$, $\forall k \in \mathcal{K}_1$ and $P_t = 40\text{dBm}$. The UAV is assumed to serve users within a radius of $R = 300\text{ m}$ at an altitude of $H = 130\text{ m}$ with $N_t = 4$. Furthermore, the $K = 4$ users are randomly located within the coverage area of each UAV-BS. A channel estimation error variance of $\zeta = 10^{-3}$ is assumed and the additive noise at the receivers is considered to have a normalized power of $\sigma^2 = \sigma_e^2 = 0\text{ dBm}$, and the minimum required transmission rate $r_c = 1$. For simplicity, we collect all the simulation parameters in table III. We compare the following SRUS protocols for the design of \mathcal{K}_1 and \mathcal{K}_2 :

- **Scheme 1: 1 Optimal Relay (1OR):** the optimal relaying protocol where the SRUS is carried out centrally at the UAV-BS by enumerating all possible relaying user combinations. The scheduling scheme having the highest max-min secrecy rate is selected. It achieves the upper bound of the max-min secrecy rate of all relaying protocols but has the highest selection complexity.

TABLE III
LIST OF SIMULATION PARAMETERS

Parameter	Value	Parameter	Value
δ	10^{-2}	K	4
$\mathcal{L}_{n,k}^i$	2	ζ	10^{-3}
$\mathcal{N}_{n,k}^i$	3.5	$\sigma^2 = \sigma_e^2$	0 dBm
P_t	40 dBm	r_c	1
R	300 m	#Iterations	25
H	130 m	N_t	4

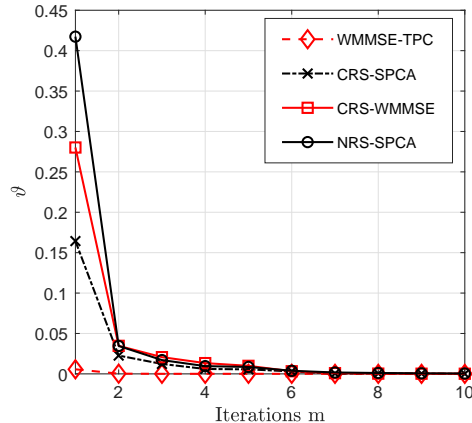


Fig. 3. Evaluating of convergence speed of the proposed FIPSA versus the number of iterations, $P_t = 40\text{ dBm}$, $N_t = 4$ and $K = 4$.

- **Scheme 2: 1 Best Relay (1BR):** the proposed SRUS protocols when $|\mathcal{K}_1| = 1$.
- **Scheme 3: $\frac{K}{2}$ Best Relays ($\frac{k}{2}$ BR):** the proposed SRUS when $|\mathcal{K}_1| = |\mathcal{K}_2|$.
- **Scheme 4: 1 Random Relay (1RR):** the UAV-BS randomly selects one user from \mathcal{K} and broadcasts the decision to all users via the “RTS” packet. It has the lowest selection complexity.

After SRUS both \mathcal{K}_1 and \mathcal{K}_2 are determined. Then we compare the following TPC, message split and time resource allocation algorithms:

- **Algorithm 1: CRS-SPCA:** the CRS model proposed in Section II and the proposed SPCA-based algorithm is adopted to solve problem (50).
- **Algorithm 2: CRS-WMMSE:** the CRS model proposed in Section II, but the optimization problem (50) is solved using the WMMSE algorithm of [19] employing one-dimensional exhaustive search for θ .
- **Algorithm 3: NRS-SPCA:** Non-CRS is also a specific instance of the CRS-SPCA scheme, when θ is fixed to 1. This is the RS scheme that has been investigated in [19], [32] for MISO BC without cooperative transmission. The transmission is completed at the end of the direct transmission phase and the cooperative transmission is blocked.
- **Algorithm 4: WMMSE-TPC:** the traditional multi-user linear TPC-based beamformer investigated in [36]. There is no RS and no cooperative transmission (i.e., $\|\mathbf{p}_c\| = 0$).

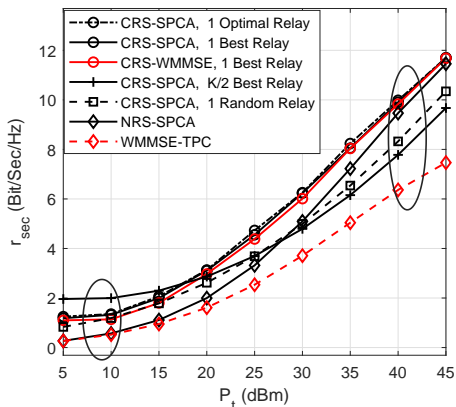


Fig. 4. The r_{sec} versus P_t comparison of different strategies, with $N_t = 4$ and $K = 4$.

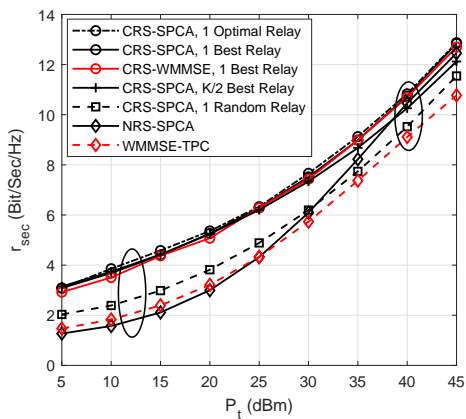


Fig. 5. The r_{sec} versus P_t comparison of different strategies, with $N_t = 8$ and $K = 4$.

and $\theta = 1$).

The TPC initialization of the WMMSE algorithm is the same as that of the proposed SPCA-based algorithm, where θ is searched with increment $\Delta\theta = 0.1$ in the CRS, WMMSE algorithm. Therefore, the precoders and message split are optimized by using the WMMSE algorithm 10 times for each value of θ selected from the set $[0.1, 0.2, \dots, 1]$. The MATLAB Toolbox *cvx* is used to solve the problem (50).

Fig. 3 depicts the average convergence of the proposed FIPSA for CRS-SPCA, CRS-WMMSE, WMMSE-TPC, and NRS-SPCA algorithms using the OF value of (51), ϑ versus the number of iterations. As observed, the average convergence speed of all algorithms are fast and converge within a few iterations. Though the proposed FIPSA algorithm is able to converge quickly within a few iterations. This is similar to the convergence speed of WMMSE.

Fig. 4 and 5 show the WCSR, r_{sec} achieved by the different strategies versus the total power budget P_t for $N_t = 4$ and 8 UAV-BS transmit antennas. As expected r_{sec} is increased with P_t . We can also observe in Fig. 4 that given a total power becomes high, the r_{sec} is increased. We can also observe that given a specific total power budget P_t , BR has almost the

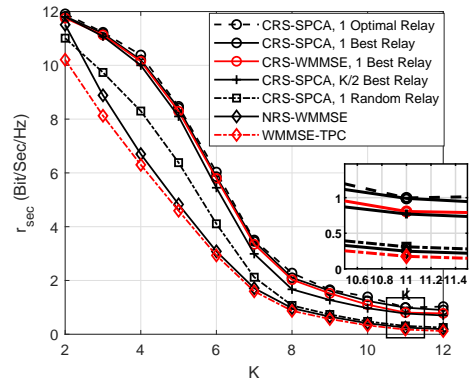


Fig. 6. The r_{sec} versus K comparison of different strategies, with $P_t = 40$ dBm and $N_t = 4$.

same performance for the proposed CRS-SPCA algorithm as OR. A comparison shows that $\frac{K}{2}$ BR, which is the same as 2BR when $K = 4$, does have a negative effect on WCSR and has a similar performance to the baseline IRR. To enhance the WCSR among users, reducing the size of \mathcal{K}_1 is preferred, because then more users can benefit from the cooperative transmission. Under the given 1BR scheduling protocol, we compare the algorithms of optimizing the RSMA TPCs, message split variables, time slot sharing and power allocation. Fig. 4 shows that the proposed CRS-SPCA algorithm performs similarly or even better in terms of WCSR than all the existing transmission schemes.

According to Fig. 5, for $N_t = 8$ the relative WCSR gain of the proposed CRS-SPCA increases, because CRS provides improved interference management capabilities, when the multi-user interference is strong.

Additionally, we see that when the number of transmit antennas N_t gets decreased, the WCSR difference between the suggested CRS-SPCA (with 1BR) and WMMSE-TPC increases, which it implies that TPC-based beamformer is only appropriate for under-loaded conditions. As N_t decreases, it is unable to handle the multi-user interference caused by all other users. In comparison, as RS-aided transmission approaches can partially decode the interference and partially treat interference as noise, they are more tolerant to the network load. A higher disparity in channel strength results in a more severe loss of common rate. By re-transmitting the s_c to the worst-case user in CRS, improves C_k^c considerably. Therefore, θ is substantially closer to 1 when user channel strength disparities are negligible. As a result, the advantages of using CRS over NRS decrease.

Fig. 6 depicts the WCSR r_{sec} versus the number of users K . Since $\sum_{k=1}^K \binom{K}{k}$ scheduling groups must be considered for obtaining the optimal SRUS, the complexity escalates as K increases. We observe that in the K -user CRS-assisted transmission network using a single SRUS-based protocol would suffice.

As shown in Fig. 6, the gap rate between NRS and CRS clearly increases as the number of users increases. It follows that as the number of users grows, the ideal theta decreases. This is

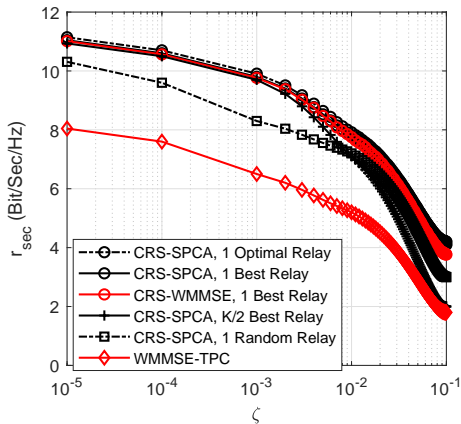


Fig. 7. The r_{sec} versus ζ comparison of different strategies, with $P_t = 40\text{dBm}$ and $N_t = 4$.

due to the fact that the multi-user interference increases with the number of users, and a larger portion of the user messages $\mathcal{W}_k|_{k=1}^K$ is transmitted via the common stream s_c . On the other hand, then *Eve* is more likely to eavesdrop successfully on the common stream which leads to a lower WCSR.

To illustrate the robustness of our proposed framework against imperfect E-CSIT, we have produced Fig. 7, where the average WCSR is depicted versus the E-CSIT estimation error ζ . Observe that regardless of the value of ζ , comparing the WCSR of the proposed CRS-SPCA scheme to that of WMMSE-TPC demonstrates the superiority of the CRS-aided transmission scheme over traditional linear TPC-based beamformer. Additionally, the WCSR performances of the various scheduling relaying protocols are similar to each other for low E-CSIT estimation error of ζ , but at high values of ζ , “ $\frac{K}{2}$ BR” performs about 50% worse than “1BR.”

Finally, Fig. 8 shows the WCSR achieved by the proposed framework versus the θ using the “1BR” method. In this experiment we aim for observing the impact of the UAV-BS altitude H and θ on the achievable WCSR r_{sec} . It is interesting to note that the r_{sec} vs. θ curve is concave, and there is an optimum θ^* at which the r_{sec} will be maximized. This figure also indicates that the WCSR critically depends on the altitude of the UAV-BS. As the height of the UAV-BS increases, the value of θ becomes closer to 1. This is because, owing to the LoS links, the quality of the common signal received at CEU is good enough at the optimal altitude H^* . Hence no cooperation is needed for relaying the common stream. In Fig. 8, increasing the height H and moving away from the optimal altitude H^* results in approximately similar distances between the UAV-BS and all users, hence the WCSR is reduced due to its higher path-loss component. By contrast, when the height of the UAV-BS is reduced from its optimal value, θ^* decreases as well due to the emergence of fading. As a result, the CEU’s common signal is adversely affected, and reliance on the cooperative phase becomes essential.

VI. CONCLUSION

To conclude, we studied the robust and secure max-min fairness of cooperative multi-user RSMA in a MISO-BC UAV

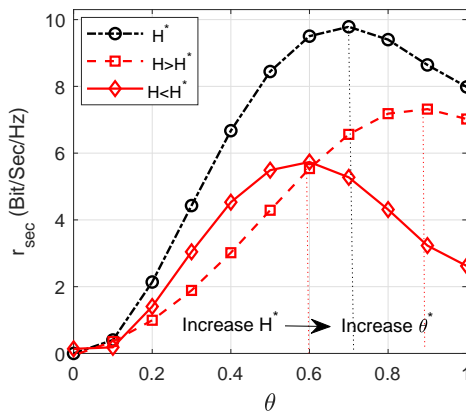


Fig. 8. The WCSR versus θ comparison of different H , with $P_t = 40\text{dBm}$ and $N_t = 4$.

network downlink where only imperfect E-CSIT is available. We formulated the problem of maximizing the WCSR by jointly optimizing the SRUS and the network’s resources allocation, including the TPCs, time slot sharing and power allocation. To circumvent the non-convexity resulting from the discrete nature of the SRUS, we proposed a two-stage algorithm, where the SRUS and network resources optimization were performed in two consecutive stages. As for the SRUS, we analytically showed that we only need the ratio of the UAV-BS $\rightarrow \{U_k|_{k \in \mathcal{K}}\}$ and $\{U_k|_{k \in \mathcal{K}}\} \rightarrow \{Eve\}$ channel gains for two type of centralized and distributed protocols. On the other hand, an SPCA-based solution has been proposed to cope with the resultant non-convexity imposed by the network resource allocation. Our numerical results show that by applying the proposed solution, the WCSR is substantially boosted over that of the benchmarks. Thus, we conclude that our cooperative multi-user RSMA framework is capable of improving the confidentiality of 6G networks.

APPENDIX A

PROOF OF PROPOSITION 3

We first prove the equivalence of the common secrecy rate achieved by users in \mathcal{K}_1 and \mathcal{K}_2 at the globally optimal point (19) by the method of contradiction. By assuming that $k_{1,min}$ and $k_{2,min}$ are the two users that respectively achieve the worst common secrecy rate in \mathcal{K}_1 and \mathcal{K}_2 at the globally optimal point $(\mathbf{P}^*, \theta^*, \mathcal{X}^*, \mathcal{K}_1^*, \{p_j^*\}_{\forall j \in \mathcal{K}_1^*}, p_z^*)$, we obtain (52), where

$$\gamma_{c,n}^{(1)}(\mathbf{P}^*) \triangleq \log_2 \left(1 + \frac{|\mathbf{h}_n^H \mathbf{p}_c^*|^2}{\sum_{k \in \mathcal{K}} |\mathbf{h}_n^H \mathbf{p}_k^*|^2 + \sigma_n^2} \right), \quad (53)$$

$$\gamma_{c,n}^{(2)}(\{p_j^*\}_{\forall j \in \mathcal{K}_1^*}, p_z^*, \mathcal{K}_1^*) \triangleq \log_2 \left(1 + \frac{\sum_{j \in \mathcal{K}_1^*} p_j^* |h_{j,n}|^2}{p_z^* |\mathbf{h}_n^H \hat{\mathbf{p}}_z|^2 + \sigma_n^2} \right) \quad (54)$$

Note that for the weakest legitimate user in \mathcal{K}_2 , i.e., $U_{k_{2,min}}$, we must have $\gamma_{c,k_{2,min}}^{\text{sec}(1)}(\mathbf{P}^*) <$

$$\mathcal{R}_{c,\mathcal{K}_1}^{\text{sec}^*} \triangleq \theta^* \left[\gamma_{c,k_1,\min}^{(1)}(\mathbf{P}^*) - \gamma_{c,e}^{(1)} \right]^+ = \theta^* \gamma_{c,k_1,\min}^{\text{sec}(1)}(\mathbf{P}^*), \quad (52)$$

$$\begin{aligned} \mathcal{R}_{c,\mathcal{K}_2}^{\text{sec}^*} &\triangleq \theta^* \left[\gamma_{c,k_2,\min}^{(1)}(\mathbf{P}^*) - \gamma_{c,e}^{(1)} \right]^+ + (1 - \theta^*) \left[\gamma_{c,k_2,\min}^{(2)}(\{p_j^*\}_{\forall j \in \mathcal{K}_1^*}, p_z^*, \mathcal{K}_1^*) - \gamma_{c,e}^{(2)} \right]^+ \\ &= \theta^* \gamma_{c,k_2,\min}^{\text{sec}(1)}(\mathbf{P}^*) + (1 - \theta^*) \gamma_{c,k_2,\min}^{\text{sec}(2)}(\{p_j^*\}_{\forall j \in \mathcal{K}_1^*}, p_z^*, \mathcal{K}_1^*), \\ &= \theta^* \left(\gamma_{c,k_2,\min}^{\text{sec}(1)}(\mathbf{P}^*) - \gamma_{c,k_2,\min}^{\text{sec}(2)}(\{p_j^*\}_{\forall j \in \mathcal{K}_1^*}, p_z^*, \mathcal{K}_1^*) \right) + \gamma_{c,k_2,\min}^{\text{sec}(2)}(\{p_j^*\}_{\forall j \in \mathcal{K}_1^*}, p_z^*, \mathcal{K}_1^*), \end{aligned}$$

$$\theta^* \gamma_{c,k_1,\min}^{\text{sec}(1)}(\mathbf{P}^*) > \theta^* \left(\gamma_{c,k_2,\min}^{\text{sec}(1)}(\mathbf{P}^*) - \gamma_{c,k_2,\min}^{\text{sec}(2)}(\{p_j^*\}_{\forall j \in \mathcal{K}_1^*}, p_z^*, \mathcal{K}_1^*) \right) + \gamma_{c,k_2,\min}^{\text{sec}(2)}(\{p_j^*\}_{\forall j \in \mathcal{K}_1^*}, p_z^*, \mathcal{K}_1^*) \quad (55)$$

$$\Leftrightarrow \theta^* > \frac{\gamma_{c,k_2,\min}^{\text{sec}(2)}(\{p_j^*\}_{\forall j \in \mathcal{K}_1^*}, p_z^*, \mathcal{K}_1^*)}{\gamma_{c,k_1,\min}^{\text{sec}(1)}(\mathbf{P}^*) - \gamma_{c,k_2,\min}^{\text{sec}(1)}(\mathbf{P}^*) + \gamma_{c,k_2,\min}^{\text{sec}(2)}(\{p_j^*\}_{\forall j \in \mathcal{K}_1^*}, p_z^*, \mathcal{K}_1^*)} = \bar{\theta}, \quad (56)$$

$$\theta^* \left[\gamma_{c,k_1,\min}^{(1)}(\mathbf{P}^*) - \gamma_{c,e}^{(1)} \right]^+ = \theta^* \left[\gamma_{c,k_2,\min}^{(1)}(\mathbf{P}^*) - \gamma_{c,e}^{(1)} \right]^+ + (1 - \theta^*) \left[\gamma_{c,k_2,\min}^{(2)}(\{p_j^*\}_{\forall j \in \mathcal{K}_1^*}, p_z^*, \mathcal{K}_1^*) - \gamma_{c,e}^{(2)} \right]^+, \quad (57)$$

$$\theta^* \left[\gamma_{c,k_1,\min}^{(1)} - \gamma_{c,k_2,\min}^{(1)} \right] = (1 - \theta^*) \left[\gamma_{c,k_2,\min}^{(2)} - \gamma_{c,e}^{(2)} \right]^+, \quad R_{c,\mathcal{K}_1}^* - R_{c,\mathcal{K}_2}^{*(1)} = \mathcal{R}_{c,\mathcal{K}_2}^{\text{sec}^*}, \quad (58)$$

$\gamma_{c,k_2,\min}^{\text{sec}(2)}(\{p_j^*\}_{\forall j \in \mathcal{K}_1^*}, p_z^*, \mathcal{K}_1^*)$ when $0 < \theta^* < 1$. Otherwise, both $\mathcal{R}_{c,\mathcal{K}_1}^{\text{sec}^*}$ and $\mathcal{R}_{c,\mathcal{K}_2}^{\text{sec}^*}$ are increasing functions of θ for the optimal \mathbf{P}^* , $\{p_j^*\}_{\forall j \in \mathcal{K}_1^*}$, p_z^* , \mathcal{K}_1^* , and the optimal θ^* should be 1 in order to maximize the minimum secrecy rate among users (**Note:** $\theta^* < 1$ means that there are some users, i.e., $\mathcal{K}_2^* \neq \phi$, that can not receive the common message with good quality and hence have to receive it in the cooperative phase. Hence, when $0 < \theta < 1$, $\mathcal{R}_{c,\mathcal{K}_1}^{\text{sec}^*}$ is a monotonically increasing function of θ , while $\mathcal{R}_{c,\mathcal{K}_2}^{\text{sec}^*}$ is a monotonic decreasing function of θ).

Proof: If at the θ^* , we assume $\mathcal{R}_{c,\mathcal{K}_1}^{\text{sec}^*} > \mathcal{R}_{c,\mathcal{K}_2}^{\text{sec}^*}$, then we have (55) and (56).

By decreasing θ from θ^* to $\bar{\theta}$, we have $\mathcal{R}_{c,2}^{\text{sec}^*}(\bar{\theta}) > \mathcal{R}_{c,2}^{\text{sec}^*}(\theta^*)$ and $\mathcal{R}_{c,1}^{\text{sec}^*}(\bar{\theta}) = \mathcal{R}_{c,1}^{\text{sec}^*}(\theta^*)$. Then the achievable common secrecy rate of $\sum_{\forall k \in \mathcal{K}} \bar{C}_k^{\text{sec}} = \min\{\mathcal{R}_{c,1}^{\text{sec}^*}(\bar{\theta}), \mathcal{R}_{c,2}^{\text{sec}^*}(\bar{\theta})\}$ increases. By allocating the improved common secrecy rate to the worst-case user, the value of the objective function achieved by using the new solution $(\mathbf{P}^*, \bar{\theta}, \bar{\chi}, \mathcal{K}_1^*, \{p_j^*\}_{\forall j \in \mathcal{K}_1^*}, p_z^*)$ is higher than that of $(\mathbf{P}^*, \theta^*, \chi^*, \mathcal{K}_1^*, \{p_j^*\}_{\forall j \in \mathcal{K}_1^*}, p_z^*)$, which contradicts to the fact that $(\mathbf{P}^*, \theta^*, \chi^*, \mathcal{K}_1^*, \{p_j^*\}_{\forall j \in \mathcal{K}_1^*}, p_z^*)$ is the globally optimal point. Similarly, we obtain that if $\mathcal{R}_{c,\mathcal{K}_1}^{\text{sec}^*} < \mathcal{R}_{c,\mathcal{K}_2}^{\text{sec}^*}$, $\theta^* < \bar{\theta}$ holds. A better solution is obtained by decreasing θ from θ^* to $\bar{\theta}$, and then a contradiction arises. Hence, we draw the conclusion that at the globally optimal point $(\mathbf{P}^*, \theta^*, \chi^*, \mathcal{K}_1^*, \{p_j^*\}_{\forall j \in \mathcal{K}_1^*}, p_z^*)$ of problem (18), $\mathcal{R}_{c,\mathcal{K}_1}^{\text{sec}^*} = \mathcal{R}_{c,\mathcal{K}_2}^{\text{sec}^*}$. As $\min_{k \in \mathcal{K}_2^*} \left\{ \mathcal{R}_{c,k}^{\text{sec}(1)} + \mathcal{R}_{c,k}^{\text{sec}(2)} \right\} \geq \min_{k \in \mathcal{K}_2^*} \left\{ \mathcal{R}_{c,k}^{\text{sec}(1)} \right\} + \min_{k \in \mathcal{K}_2^*} \left\{ \mathcal{R}_{c,k}^{\text{sec}(2)} \right\}$, we obtain that $\mathcal{R}_{c,\mathcal{K}_2}^{\text{sec}^*} > \min_{k \in \mathcal{K}_2^*} \left\{ \mathcal{R}_{c,k}^{\text{sec}(1)} \right\}$.

Based on (19), we have $\mathcal{R}_{c,\mathcal{K}_1}^{\text{sec}^*} > \min_{k \in \mathcal{K}_2^*} \left\{ \mathcal{R}_{c,k}^{\text{sec}(1)} \right\}$ when $0 < \theta^* < 1$ and the proof of proposition 1 is completed. ■

APPENDIX B PROOF OF PROPOSITION 5

SPCA ensures monotonic improvement of r_{sec} , i.e., $r_{\text{sec}}^{[n]} \geq r_{\text{sec}}^{[n+1]}$. This is due to the fact that the solution generated by solving problem (23) at iteration $[n-1]$ is a feasible point of problem (23) at iteration $[n]$. Due to the transmit power constraint ((18)-C₄), the sequence $\left\{ r_{\text{sec}}^{[n]} \right\}_{n=1}^{\infty}$ is bounded from above, which implies that the convergence of the proposed SPCA-based algorithm is guaranteed. Next, we show that the sequence of $(\mathbf{P}^{[n]}, \theta^{[n]}, \chi^{[n]}, \{p_j^{[n]}\}_{\forall j \in \mathcal{K}_1^*}, \beta_{\{c,e,p\}}^{[n]}, \rho_{\{c,p\}}^{[n]}, \alpha_{c,e}^{[n]})$ converges to the set of stationary points of problem (23). The proposed SPCA-based algorithm is in fact an inner approximation algorithm of the non-convex optimization literature [30], [31]. This is proved by showing the equivalence of the KKT conditions of problem (22) and problem (23) when the solution $(\mathbf{P}, \theta, \chi, \{p_j\}_{\forall j \in \mathcal{K}_1^*}, \beta_{\{c,e,p\}}, \rho_{\{c,p\}}, \alpha_{c,e})$ is equal to $(\mathbf{P}^{[n]}, \theta^{[n]}, \chi^{[n]}, \{p_j^{[n]}\}_{\forall j \in \mathcal{K}_1^*}, \beta_{\{c,e,p\}}^{[n]}, \rho_{\{c,p\}}^{[n]}, \alpha_{c,e}^{[n]})$. Combined with the fact that the Taylor approximations made in (23) are asymptotically tight as $n \rightarrow \infty$ [31], we can see that the solution of the proposed SPCA-based algorithm converges to the set of KKT points (which are also known as the stationary points) of problem (22).

REFERENCES

- [1] M. Z. Chowdhury, M. Shahjalal, S. Ahmed, and Y. M. Jang, "6g wireless communication systems: Applications, requirements, technolo-

- gies, challenges, and research directions," *IEEE Open Journal of the Communications Society*, vol. 1, pp. 957–975, 2020.
- [2] K. Sheth, K. Patel, H. Shah, S. Tanwar, R. Gupta, and N. Kumar, "A taxonomy of AI techniques for 6G communication networks," *Computer communications*, vol. 161, pp. 279–303, 2020.
- [3] Y. Liu, S. Zhang, X. Mu, Z. Ding, R. Schober, N. Al-Dhahir, E. Hossain, and X. Shen, "Evolution of NOMA toward next generation multiple access (NGMA) for 6G," *IEEE Journal on Selected Areas in Communications*, 2022.
- [4] O. Dizdar, Y. Mao, W. Han, and B. Clerckx, "Rate-splitting multiple access: A new frontier for the PHY layer of 6G," in *2020 IEEE 92nd Vehicular Technology Conference (VTC2020-Fall)*, pp. 1–7, IEEE, 2020.
- [5] O. Dizdar, Y. Mao, Y. Xu, P. Zhu, and B. Clerckx, "Rate-splitting multiple access for enhanced URLLC and EMBB in 6G," in *2021 17th International Symposium on Wireless Communication Systems (ISWCS)*, pp. 1–6, IEEE, 2021.
- [6] P. Porambage, G. G`ur, D. P. M. Osorio, M. Liyanage, A. Gurtov, and M. Ylianttila, "The roadmap to 6G security and privacy," *IEEE Open Journal of the Communications Society*, vol. 2, pp. 1094–1122, 2021.
- [7] C. Lipps, S. Baradie, M. Noushinfar, J. Herbst, A. Weinand, and H. D. Schotten, "Towards the sixth generation (6G) wireless systems: Thoughts on physical layer security," in *Mobile Communication-Technologies and Applications: 25th ITG-Symposium*, pp. 1–6, VDE, 2021.
- [8] S. E. Zegrar, H. M. Furqan, and H. Arslan, "Flexible physical layer security for joint data and pilots in future wireless networks," *IEEE Transactions on Communications*, vol. 70, no. 4, pp. 2635–2647, 2022.
- [9] H. Bastami, M. Moradikia, H. Behroozi, R. C. de Lamare, A. Abdelhadi, and Z. Ding, "Secrecy rate maximization for hardware impaired untrusted relaying network with deep learning," *Physical Communication*, vol. 49, p. 101476, 2021.
- [10] M. Moradikia, H. Bastami, A. Kuhestani, H. Behroozi, and L. Hanzo, "Cooperative secure transmission relying on optimal power allocation in the presence of untrusted relays, a passive eavesdropper and hardware impairments," *IEEE Access*, vol. 7, pp. 116942–116964, 2019.
- [11] L. Hu, H. Wen, B. Wu, F. Pan, R.-F. Liao, H. Song, J. Tang, and X. Wang, "Cooperative jamming for physical layer security enhancement in Internet of Things," *IEEE Internet of Things Journal*, vol. 5, no. 1, pp. 219–228, 2017.
- [12] H. Bastami, M. Letafati, M. Moradikia, A. Abdelhadi, H. Behroozi, and L. Hanzo, "On the physical layer security of the cooperative rate-splitting-aided downlink in UAV networks," *IEEE Transactions on Information Forensics and Security*, vol. 16, pp. 5018–5033, 2021.
- [13] H. Bastami, M. Moradikia, A. Abdelhadi, H. Behroozi, B. Clerckx and L. Hanzo, "Maximizing the Secrecy Energy Efficiency of the Cooperative Rate-Splitting Aided Downlink in Multi-Carrier UAV Networks," in *IEEE Transactions on Vehicular Technology*, 2022, doi: 10.1109/TVT.2022.3192298.
- [14] J. Tang, L. Jiao, K. Zeng, H. Wen and K. Y. Qin, "Physical Layer Secure MIMO Communications Against Eavesdroppers With Arbitrary Number of Antennas," in *IEEE Transactions on Information Forensics and Security*, vol. 16, pp. 466–481, 2021, doi: 10.1109/TIFS.2020.3015548.
- [15] Z. Tang, T. Hou, Y. Liu, J. Zhang and L. Hanzo, "Physical Layer Security of Intelligent Reflective Surface Aided NOMA Networks," in *IEEE Transactions on Vehicular Technology*, vol. 71, no. 7, pp. 7821–7834, July 2022, doi: 10.1109/TVT.2022.3168392.
- [16] P. Li, M. Chen, Y. Mao, Z. Yang, B. Clerckx, and M. Shikh-Bahaei, "Cooperative rate-splitting for secrecy sum-rate enhancement in multi-antenna broadcast channels," in *2020 IEEE 31st Annual International Symposium on Personal, Indoor and Mobile Radio Communications*, pp. 1–6, IEEE, 2020.
- [17] H. Fu, S. Feng, W. Tang, and D. W. K. Ng, "Robust secure beamforming design for two-user downlink MISO rate-splitting systems," *IEEE Transactions on Wireless Communications*, vol. 19, no. 12, pp. 8351–8365, 2020.
- [18] J. An, O. Dizdar, B. Clerckx, and W. Shin, "Rate-splitting multiple access for multi-antenna broadcast channel with imperfect CSIT and CSIR," *arXiv preprint arXiv:2102.08738*, 2021.
- [19] J. Zhang, B. Clerckx, J. Ge and Y. Mao, "Cooperative Rate Splitting for MISO Broadcast Channel with User Relaying, and Performance Benefits Over Cooperative NOMA," in *IEEE Signal Processing Letters*, vol. 26, no. 11, pp. 1678–1682, Nov. 2019.
- [20] Y. Mao, B. Clerckx, and V. O. Li, "Rate-splitting multiple access for downlink communication systems: bridging, generalizing, and outperforming SDMA and NOMA," *EURASIP journal on wireless communications and networking*, vol. 2018, no. 1, p. 133, 2018.
- [21] Y. Mao, B. Clerckx, J. Zhang, V.O. Li, and M. A. Arafah, "Max-min fairness of K-user cooperative rate-splitting in MISO broadcast channel with user relaying," *IEEE Transactions on Wireless Communications* 19, no. 10 (2020): 6362–6376.
- [22] L. Xiao, Y. Xu, D. Yang and Y. Zeng, "Secrecy Energy Efficiency Maximization for UAV-Enabled Mobile Relaying," in *IEEE Transactions on Green Communications and Networking*, vol. 4, no. 1, pp. 180–193, March 2020.
- [23] S. Ahmed, M. Z. Chowdhury, S. R. Sabuj, M. I. Alam and Y. M. Jang, "Energy-Efficient UAV Relaying Robust Resource Allocation in Uncertain Adversarial Networks," in *IEEE Access*, vol. 9, pp. 59920–59934, 2021.
- [24] W. Jaafar, S. Naser, S. Muhaidat, P. C. Sofotasios and H. Yanikomeroğlu, "On the Downlink Performance of RSMA-Based UAV Communications," in *IEEE Transactions on Vehicular Technology*, vol. 69, no. 12, pp. 16258–16263, Dec. 2020.
- [25] H. Zhang, J. Zhang and K. Long, "Energy Efficiency Optimization for NOMA UAV Network With Imperfect CSI," in *IEEE Journal on Selected Areas in Communications*, vol. 38, no. 12, pp. 2798–2809, Dec. 2020.
- [26] Li, Sixian, Bin Duo, Marco Di Renzo, Meixia Tao, and Xiaojun Yuan. "Robust secure UAV communications with the aid of reconfigurable intelligent surfaces." *IEEE Transactions on Wireless Communications* 20, no. 10 (2021): 6402–6417.
- [27] H. Bastami, M. Moradikia, M. Letafati, A. Abdelhadi, and H. Behroozi. "Outage-Constrained Robust and Secure Design for Downlink Rate-Splitting UAV Networks." In *2021 IEEE International Conference on Communications Workshops (ICC Workshops)*, pp. 1–7. IEEE, 2021.
- [28] H. Fu, S. Feng, W. Tang and D. W. K. Ng, "Robust Secure Beamforming Design for Two-User Downlink MISO Rate-Splitting Systems," in *IEEE Transactions on Wireless Communications*, vol. 19, no. 12, pp. 8351–8365, Dec. 2020.
- [29] E. Boshkovska, D. W. K. Ng, N. Zlatanov, A. Koelpin and R. Schober, "Robust resource allocation for MIMO wireless powered communication networks based on a non-linear EH model," in *IEEE Transactions on Communications*, vol. 65, no. 5, pp. 1984–1999, May 2017.
- [30] B. R. Marks and G. P. Wright, "A general inner approximation algorithm for nonconvex mathematical programs," *Oper. Res.*, vol. 26, no. 4, pp. 681–683, 1978.
- [31] W. Li, T. Chang, C. Lin, and C. Chi, "Coordinated beamforming for multiuser MISO interference channel under rate outage constraints," *IEEE Trans. Signal Process.*, vol. 61, no. 5, pp. 1087–1103, March 2013.
- [32] B. Clerckx, H. Joudeh, C. Hao, M. Dai, and B. Rassouli, "Rate splitting for MIMO wireless networks: A promising PHY-layer strategy for LTE evolution," *IEEE Commun. Mag.*, vol. 54, no. 5, pp. 98–105, May 2016.
- [33] Y. Yang, M. Ma, S. Aïssa and L. Hanzo, "Physical-Layer Secret Key Generation via CQI-Mapped Spatial Modulation in Multi-Hop Wiretap Ad-Hoc Networks," in *IEEE Transactions on Information Forensics and Security*, vol. 16, pp. 1322–1334, 2021.
- [34] Z. Kong, S. Yang, D. Wang and L. Hanzo, "Robust Beamforming and Jamming for Enhancing the Physical Layer Security of Full Duplex Radios," in *IEEE Transactions on Information Forensics and Security*, vol. 14, no. 12, pp. 3151–3159, Dec. 2019.
- [35] Z. Kong, J. Song, C. Wang, H. Chen and L. Hanzo, "Hybrid Analog Digital Precoder Design for Securing Cognitive Millimeter Wave Networks," in *IEEE Transactions on Information Forensics and Security*, 2020.
- [36] S. S. Christensen, R. Agarwal, E. D. Carvalho, and J. M. Cioffi, "Weighted sum-rate maximization using weighted MMSE for MIMO-BC beamforming design," *IEEE Trans. Wireless Commun.*, vol. 7, no. 12, pp. 4792–4799, Dec 2008.
- [37] S. Boyd and L. Vandenberghe, *Convex optimization*. Cambridge University Press, 2004.
- [38] O. Tervo, L. N. Tran, and M. Juntti, "Optimal energy-efficient transmit beamforming for multi-user MISO downlink," *IEEE Trans. Signal Process.*, vol. 63, no. 20, pp. 5574–5588, Oct 2015.
- [39] A. Beck, A. Ben-Tal, and L. Tetrushvili, "A sequential parametric convex approximation method with applications to nonconvex truss topology design problems," *Journal of Global Optimization*, vol. 47, no. 1, pp. 29–51, May 2010. [Online]. Available: <https://doi.org/10.1007/s10898-009-9456-5>